

Data report: dissolved minor element compositions, sediment major and minor element concentrations, and reactive iron and manganese data from the Lesser Antilles volcanic arc region, IODP Expedition 340 Sites U1394, U1395, U1396, U1399, and U1400¹

Natalie A. Murray,² Jesse M. Muratli,³ Anne M. Hartwell,² Hayley Manners,⁴ Meghan R. Megowan,³ Miguel Goñi,³ Martin Palmer,⁵ and James McManus^{2, 6}

Chapter contents

Abstract	1
Introduction	1
Analytical methods	2
Results	4
Acknowledgments	5
References	5
Figures	7
Tables	18

¹Murray, N.A., Muratli, J.M., Hartwell, A.M., Manners, H., Megowan, M.R., Goñi, M., Palmer, M., and McManus, J., 2016. Data report: dissolved minor element compositions, sediment major and minor element concentrations, and reactive iron and manganese data from the Lesser Antilles volcanic arc region, IODP Expedition 340 Sites U1394, U1395, U1396, U1399, and U1400. In Le Friant, A., Ishizuka, O., Stroncik, N.A., and the Expedition 340 Scientists, *Proceedings of the Integrated Ocean Drilling Program*, 340: Tokyo (Integrated Ocean Drilling Program Management International, Inc.).

doi:10.2204/iodp.proc.340.207.2016

²The University of Akron, Department of Geosciences, Akron OH 44235, USA.

³Oregon State University, College of Earth, Ocean, and Atmospheric Sciences, Corvallis OR 97331, USA.

⁴University of Plymouth, School of Geography, Earth and Environmental Sciences, Plymouth, Devon PL4 8AA, United Kingdom.

⁵National Oceanography Centre Southampton, Southampton SO14 3ZH, United Kingdom.

⁶Present address: Bigelow Laboratory for Ocean Sciences, 60 Bigelow Drive, P.O. Box 380, East Boothbay ME 04544, USA. Correspondence author: jmcmanus@bigelow.org

Abstract

We measured dithionite-extractable iron and manganese along with a variety of bulk sedimentary solid and dissolved phases to constrain diagenetic reactions occurring within the sediment package of Grenada Basin, which is within the Lesser Antilles volcanic arc region. Core material was obtained during Integrated Ocean Drilling Program Expedition 340. For this report we focus primarily on five sites; three sites are located in the northern portion of the study area off the island of Montserrat (Sites U1394–U1396), and two sites are located farther south off the island of Martinique (Sites U1399 and U1400). Sediments throughout this region include tephra-rich volcanic sands, hemipelagic mud sequences, and carbonate-rich sequences, with widely variable proportions over short (centimeter scale) depth intervals. Regardless of the main sediment type, organic carbon contents are low with average values of 0.19 ± 0.1 wt% at Site U1394, 0.13 ± 0.08 wt% at Site U1395, 0.13 ± 0.06 wt% at Site U1396, 0.28 ± 0.08 wt% at Site U1399, and 0.23 ± 0.15 wt% at Site U1400. Carbonate contents are more variable, ranging between 0 and ~80 wt%, in cores from Sites U1394–U1396 and between 1 and 40 wt% at both Sites U1399 and U1400. These variations in carbonate content likely reflect variable dilution with volcanogenic sediment. Pore fluids reflect a range of diagenetic conditions from oxidizing (sulfate rich) to sulfate-reducing conditions. Reactive major elements (Ca and Mg) as well as a number of minor elements show a range of diagenetic behaviors from reactions likely related to carbonate dissolution or precipitation to exchange reactions between pore fluids and the volcanic-rich sedimentary substrate and clay formation. However, significant site-to-site variability is seen in the diagenetic behavior of these elements. Solid-phase reactive Fe ranges from 0.18 to 0.75 wt% at the northern sites and 0.4 to 1.5 wt% at the southern sites, whereas reactive Mn ranges from 0 to 0.1 wt% in the north and 0 to 0.3 wt% in the south.

Introduction

Integrated Ocean Drilling Program (IODP) Expedition 340 cored several sites within the Lesser Antilles volcanic arc region. The



overall goal of the project was to drill volcanogenic landslides in the marine environment to establish a record of eruption cycles and the impact of these landslides on the marine sedimentary record. This report focuses on sediment geochemical results from five sites (U1394–U1396, U1399, and U1400; Fig. F1). Sites U1394–U1396 are located south of the island of Montserrat in 1115, 1191, and 801 m of water, respectively (see the “[Expedition 340 summary](#)” chapter [Expedition 340 Scientists, 2013a]). Site U1394 is located ~24 km southeast of Montserrat, whereas Site U1395 is located further southeast of Site U1394, between the islands of Montserrat and Guadeloupe (Fig. F1). The lithology of Sites U1394 and U1395 is similar and consists of hemipelagic muds, turbidite deposits, mafic volcaniclastics and volcaniclastic sands, hemipelagic mud, and tephra layers. Although Site U1396 to the west has similar sedimentation to Sites U1394 and U1395, given that this site resides on a bathymetric high our expectation is that the sediments will have a tendency toward more fine grained material; nevertheless, volcaniclastic sand, hemipelagic mud, and tephra layers all dominate this core’s lithology as well (see the “[Expedition 340 summary](#)” chapter [Expedition 340 Scientists, 2013a]; Le Friant et al., 2015; Palmer et al., 2016).

Sites U1399 and U1400 are located west of the island of Martinique in Grenada Basin in 2900 and 2745 m water depth, respectively (Fig. F1). The lithology of these two sites is similar and is composed of hemipelagic mud, interbedded tephra layers, volcaniclastic turbidites, and deformed sediments (see the “[Expedition 340 summary](#)” chapter [Expedition 340 Scientists, 2013a]; Le Friant et al., 2015). Site U1400 is located west of Martinique but closer in proximity to the island than Site U1399 (Fig. F1).

Analytical methods

Pore fluid extractions

Pore fluids were obtained from all sediment cores presented in this report (Table T1). Sampling occurred every 10 m unless the sediment was unsuitable for pore fluid extraction (i.e., because of sands, debris, or other mission-specific rationales). Sampling procedures are described in detail in the “[Methods](#)” chapter (Expedition 340 Scientists, 2013b); however, we present a brief description for completeness. A 10 to 15 cm section of whole-round core was removed to begin the squeezing process in the laboratory. Whole-round sections were processed within a nitrogen-filled bag at room temperature and then transferred to a hydraulic press for pore fluid extraction (Manheim, 1966). Following extraction,

pore fluids were filtered and subsampled for various dissolved constituents (see the “[Methods](#)” chapter [Expedition 340 Scientists, 2013b]).

Pore fluid ICP-OES and ICP-MS methods

As part of this report, we provide some previously published major element data (Ca, Mg, and SO_4^{2-}) (see the “[Expedition 340 summary](#)” and “[Methods](#)” chapters [Expedition 340 Scientists, 2013a, 2013b]) along with previously unpublished minor element data (Li, B, Sr, Si, Mn, Rb, and Cs; Table T1). For the minor elements (Li, B, Si, and Mn), samples were diluted to a 0.25:5 ratio with 1% quartz-distilled nitric acid. Strontium was measured twice, once with the major elements at 100-fold dilution and once with the minor elements at 20-fold dilution. Together, these two runs capture the full dynamic range of Sr in these samples with greater precision than either single analysis alone. Minor element standards were matrix-matched to the samples with an artificial salt water solution made to approximate seawater concentrations of Na, Mg, and Cl from ultrapure salts (Sigma Aldrich). Instrumental drift was monitored by repeated runs of the standard curve, but was not found to influence the inductively coupled plasma-optical emissions spectrometer (ICP-OES) results significantly. Individual sample values represent a mean of three replicate analyses for each element in each sample tube. Uncertainties reported here are 1σ uncertainties derived from two sources: (1) the regression uncertainty, calculated using the standard error of the regression, and (2) the “internal” uncertainty calculated from the standard deviation of the three replicate analyses. The reported uncertainties are combined as the square root of the sum of squares. Detection limits reported here are the point at which the regression uncertainty is one-third of the concentration. Above this point, the concentration measured is $>3\sigma$ above zero.

Cs and Rb samples were run on a Thermo X-Series II inductively coupled plasma–mass spectrometer (ICP-MS). ICP-MS signals can drift significantly over the course of an analytical session; therefore, instrumental drift was corrected by spiking each sample tube with an internal standard solution. This solution consisted of ~50 ppb each of Rh and Re. Measured counts throughout the run were corrected to the value of the first acid blank run of the day. Although Re was not used to correct either of the target elements, it was used as an assessment tool to monitor instrumental drift. Samples were diluted to a 0.25:5 ratio with 1% quartz-distilled nitric acid. Standards were spiked with the same artificial salt water solution as used for the minor element analysis to match the matrix of the samples. Though ultrapure salts



were used, we found this solution contained a Cs blank. We determined that the solution contained $\sim 2.5 \pm 0.1$ nmol/L in the undiluted salt water solution, and this value was used to correct the standard concentrations.

Solid-phase total digestion methods and analyses

Total sediment digestion methods are described in detail elsewhere (Muratli et al., 2012; Muratli et al., 2015). Briefly, prior to digestion sediments were dried and ground. Total sediment digestion was accomplished through a microwave-assisted (CEM MARS-5 microwave oven) digestion process that utilized the inorganic acids HCl, HNO₃, and HF (Muratli et al., 2015). Samples were diluted with 5% HNO₃ and were heated for ~ 24 h prior to analysis to remove residual fluoride complexes (Muratli et al., 2012).

To assess precision, laboratory standards (PACS-2 and an in-house standard RR9702A-42MC) were digested on multiple occasions, and $\sim 10\%$ of the samples during a run were replicated. RR9702A-42MC is an in-house Chilean margin sediment standard that our group has been using to assess long-term method precision, and PACS-2 is a marine sediment reference material (National Research Council [NRC] Canada) from the Harbour of Esquimalt, Canada.

For the solid-phase major element data (Table T2), we analyzed samples on a Leeman Laboratories Prodigy ICP-OES at the K.W. Keck Collaboratory at Oregon State University (USA), and our approach was similar to that employed for pore fluids as discussed above. Specific emission wavelengths for analysis of solid-phase digests are reported in Table T3. Samples and standards were typically diluted 20-fold with 1% quartz-distilled nitric acid. For elements affected by instrumental drift, a correction was applied. Data values are an average of three replicate analyses for each element. We report uncertainties at 1σ , which are calculated as indicated for the dissolved phases.

Dithionite-extractable Fe and Mn

A single-step mild chemical leach was performed on samples to extract the labile or “reactive” fraction of Fe and Mn from the sediments (Mehra and Jackson, 1960) (Tables T4, T5, T6). We added ~ 0.25 g of dried ground sediment to centrifuge tubes and then added ~ 10 mL of dithionite reagent. We used a sodium acetate, sodium citrate solution as a buffer (Kostka and Luther, 1994; Roy et al., 2013). Centrifuge tubes were agitated with a vortex stirrer and placed in a heating block for 4 h at 60°C. Each sample was mixed every 15 min, and at the end of 4 h samples were centri-

fuged at 4000 rpm for 5 min. Leachate was then transferred into a labeled bottle, and sample mass was recorded. For some of the samples (Sites U1399 and U1400), a precipitate or gel-like substance precipitated from solution over time. Samples that showed the presence of a precipitate were reextracted and then diluted immediately following extraction.

Analyses for reactive Fe and Mn samples (Sites U1394–U1396) were analyzed on a Leeman Labs Prodigy ICP-OES at Oregon State University (Table T4), and samples from Sites U1399 and U1400 were analyzed on a Perkin Elmer Atomic Absorption Spectrometer, AAnalyst 700, at the University of Akron (Tables T4, T5). Additional samples for Site U1396 were also analyzed at the University of Akron on an Agilent Technologies 700 series ICP-OES (Table T6). For the samples from Sites U1394–U1396 that were measured at Oregon State University, we assessed precision by using the standard reference material, PACS-2 (NRC Canada), as well as our Chilean margin laboratory standard. Reactive Fe in these two standards was measured to be 0.79 ± 0.02 wt% for the PACS-2 standard and 0.93 ± 0.02 wt% for the Chilean margin standard. For reactive Mn, the values are 0.0029 ± 0.0001 wt% and 0.0024 ± 0.0001 wt%, respectively. These values compare favorably with previous runs from our laboratory with the exception that the reactive iron values are slightly lower than the longer term average reported in Roy et al. (2013), where the reactive Fe values for PACS-2 and Chilean margin samples are 0.88 ± 0.08 wt% and 1.08 ± 0.08 wt%, respectively. The values reported for this communication are, however, consistent with those reported in Muratli et al. (2015). To assess precision for the samples from Sites U1399 and U1400 (Tables T4, T5), we used an in-house carbonate-rich laboratory standard, PACS-3 (NRC Canada), and the standard reference material 2702 (National Institute of Standards and Technology), which is a marine sediment from Baltimore Harbor. Reactive Fe for these samples was determined to be $0.71\% \pm 0.03\%$ (in-house carbonate), $0.85\% \pm 0.04\%$ (PACS-3), and $3.11\% \pm 0.08\%$ (2702), and reactive Mn is $0.16\% \pm 0.05\%$ (in-house carbonate) and $0.15\% \pm 0.05\%$ (2702). Reactive Mn for PACS-3 was not detectable.

Reproducibility for samples (Table T6) was accessed from standard reference materials PACS-3, MESS-3, and MESS-4 that were analyzed during extractions with unknown samples. Iron, manganese, and aluminum in PACS-3 are $0.89\% \pm 0.03\%$ ($N = 5$), $0.0038\% \pm 0.0008\%$ ($N = 5$), and $0.121\% \pm 0.010\%$ ($N = 3$), respectively. Fe, Mn, and Al for MESS-3 are $1.68\% \pm 0.05\%$ ($N = 5$), $0.0182\% \pm 0.0009\%$ ($N = 5$), and $0.131\% \pm 0.001\%$ ($N = 3$), respectively. Fe, Mn,

and Al in MESS-4 are $1.51\% \pm 0.07\%$ ($N = 3$), $0.0171\% \pm 0.0003\%$ ($N = 3$), and $0.143\% \pm 0.001\%$ ($N = 3$), respectively.

Organic carbon, nitrogen, and inorganic carbon

Organic carbon and nitrogen for most of the samples presented here were analyzed at Oregon State University following the methodology outlined in Gofñi et al. (2003) with minor modifications (Tables T4, T5). This technique uses 20–30 mg of sample placed into silver boats and exposed to hydrochloric vapors to remove all inorganic carbon (Hedges and Stern, 1984). Complete removal of inorganic carbon involves pipetting one to two drops of 10% HCl into the samples after vapor acidification is complete. Samples are then dried and run on a Thermo Quest EA2500 elemental analyzer. Blanks containing minor amounts of carbon but no nitrogen were analyzed. Organic carbon measurements were corrected for the amount of carbon recorded by the blanks. Inorganic carbon measurements were completed at The University of Akron on a UIC Coulometrics coulometer. The analysis required ~40 mg of sample placed in gelatin capsules. A purge of the sample flask with CO₂-free carrier gas removes atmospheric CO₂. Following the purge, 5 mL of perchloric acid (HClO₄) was added to the flask to acidify the inorganic carbon in order to determine the amount of CO₂ within the sample.

Hole U1396C tephra samples (Table T6) were freeze-dried (24 h), crushed using a granite pestle and mortar, and decarbonated using excess hydrochloric acid (10% v/v) until any visible sign of reaction had ceased. This process was followed by repeated washing with deionized water until a neutral solution was obtained, followed by freeze drying (24 h). Approximately 10 mg of decarbonated and unaltered sample was weighed into a tin cup and then was crushed and analyzed for total organic carbon (TOC) and total carbon (TC) content, respectively, using a Carlo Erba 1110 elemental analyzer with L-cysteine as the calibration standard.

Results

Pore fluids

Some pore fluid results from the expedition have been presented previously (see the “Expedition 340 summary” chapter [Expedition 340 Scientists, 2013a]), and this report contributes additional data as discussed above. Both the major (see the “Expedition 340 summary” chapter [Expedition 340 Scientists, 2013a]) and minor element data (Table T1; Figs.

F2, F3, F4, F5, F6, F7) show a variety of distributions that are likely influenced by a mixture of reactions that include organic carbon decomposition, carbonate dissolution and precipitation reactions, and volcanogenic sediment diagenesis. Ca and Mg are two of the more diagnostic elements for differentiating among these processes. For example, data from Site U1396 demonstrates Ca increases that mirror the Mg decreases (Fig. F4), which is quite likely driven by exchange reactions during diagenesis of volcanic glass (see the “Expedition 340 summary” chapter [Expedition 340 Scientists, 2013a]). By contrast, Site U1399 shows a decrease in Ca and Mg, which is likely a result, at least in part, of carbonate precipitation reactions at depth (Fig. F5). Sulfate varies from being quite close to the seawater value (~28 mM) throughout the profile (Site U1396; Fig. F4) to being depleted to ~10 mM at Site U1394 (Fig. F2). Manganese exhibits a variety of behaviors likely reflecting organic carbon oxidation reactions as well as variations in sedimentary reactive Mn content. The other elements, Si, B, Li, Sr, Rb, and Cs, all show a similar diversity in behaviors that are likely driven by these same or similar diagenetic reactions involving volcanic material, carbonate, biogenic silica, and organic matter (Figs. F2, F3, F4, F5, F6).

Whole-sediment digestion results

Whole-sediment digestion results are presented in Table T2. These results are for selected samples from Sites U1395, U1396, U1399, and U1400 and are not plotted separately, as there are too few data to construct meaningful interpretations. However, results do show considerable variability, which is consistent with the highly variable mixture of hemipelagic muds, turbidites, and volcaniclastic sediments.

Dithionite extraction results

Whole-core distributions

Dithionite-extractable iron (Fe_R) and manganese (Mn_R) as well as organic carbon (OC) generally have lower concentrations at the northern sites (Figs. F7, F8, F9) with highly variable CaCO₃ (0–81 wt%) as compared to the southern sites, which show more variation in their Fe_R, Mn_R, and OC concentrations with less variation in their CaCO₃ contents (Figs. F10, F11; Table T4).

At Site U1394, Fe_R, Mn_R, and OC have relatively low concentrations throughout the record. In the uppermost 25 m of sediment, these three components have average values of 0.39 ± 0.09 wt%, 0.03 ± 0.01 wt%, and 0.19 ± 0.1 wt%, respectively. Carbonate varies from 5 to 75 wt% within the uppermost 22 m of sediment. An ~87 m region produced no data,



which reflects the fact that fine-grained material recovery within this interval was generally poor. From 111 to 197 meters below seafloor (mbsf), Fe_R and Mn_R are relatively constant, averaging 0.37 ± 0.03 wt% and 0.03 ± 0.01 wt%, respectively (Fig. F7A, F7B). Organic carbon averages 0.23 ± 0.1 wt% (Fig. F7C), and carbonate shows less variability in its concentration (55–60 wt%) compared to the upper 22 mbsf, with the exception of three low-concentration samples (Fig. F7D).

Some of the solid-phase concentrations at Site U1395 show a wider range in concentration compared to Site U1394. Fe_R , in particular, ranges from 0.18 to 0.75 wt% throughout the core with more variability below 60 mbsf (Fig. F8A). In contrast, Mn_R is particularly low, averaging 0.02 ± 0.02 wt%, with the exception of a single data point (0.09 wt%) at ~ 100 mbsf (Fig. F8B). Organic carbon averages 0.13 ± 0.08 wt% (Fig. F8C). Calcium carbonate varies between 0 and 76 wt%, and at ~ 169 mbsf, CaCO_3 decreases from 81 to 43 wt% (Fig. F8D).

Site U1396 solid phases, with the exception of CaCO_3 , are relatively constant with depth (Fig. F9). Fe_R averages 0.35 ± 0.06 wt% with depth, with the highest sample at 0.48 wt% (Fig. F9A). Mn_R and OC are both uniformly low, averaging 0.02 ± 0.01 wt% and 0.13 ± 0.06 wt%, respectively (Fig. F9B, F9C). As is the case for Site U1395, calcium carbonate values show large variability ranging from 0 to 74 wt% throughout the core.

Site U1399 solid-phase data exhibit more variability in Fe_R , Mn_R , and OC with depth compared to Sites U1394–U1396 (Fig. F10). Fe_R has greater variability (0.46–1.4 wt%) in the uppermost 75 m of the core compared to the lowermost ~ 179 m of the core (0.42–1.06 wt%) (Fig. F10A). Mn_R is highly variable compared to the northern cores and has an average of 0.065 ± 0.046 wt% (Fig. F10B). Organic carbon ranges from 0.01 to 0.61 wt% with an average of 0.28 ± 0.15 wt% (Fig. F10C). CaCO_3 ranges from 2.5 to 36 wt% with depth, showing less variation compared to the northern sites (Fig. F10D).

Site U1400 solid-phase data are similar to those of Site U1399, with Fe_R , Mn_R , and, to a lesser extent, OC exhibiting more variation with depth and less variability in CaCO_3 compared to the northern sites (Fig. F11). Reactive Fe ranges from 0.4 to 1.4 wt% with an average of 0.8 ± 0.3 wt% (Fig. F11A). Mn_R values exhibit considerable scatter throughout the core, with an average value of 0.068 ± 0.037 wt% (Fig. F11B). Organic carbon shows a slight decrease to 200 mbsf and then increases with depth. However, OC is less abundant at Site U1400 compared to Site U1399, ranging from 0.1 to 0.4 wt% with an average of 0.23

± 0.08 wt% (Fig. F11C). Calcium carbonate ranges from 2 to 35 wt% and demonstrates increases at approximately the same depths as Mn_R (Fig. F11D).

Discrete intervals

In addition to the results presented above, we analyzed samples from Sites U1399 and U1400 from focused or discrete sedimentary intervals (Table T5). These intervals were chosen based on abrupt lithology transitions. A total of nine different sections (5–6 samples in each section) were chosen, six from Site U1399 and three from Site U1400. The different sections include (in order of increasing depth) Sections 340-U1399B-3H-3, 7H-3, 11H-2, 16H-2, 19H-2, and 25H-2 and Sections 340-U1400B-16H-2, 26H-5, and 48X-1. Solid-phase data and visual lithology descriptions can be found in Table T5, and the results are plotted on Figures F12, F13, F14, F15, F16, F17, F18, F19, and F20. The general observation is that these changes in lithology often coincide with changes in reactive Fe and Mn as well as with OC and carbonate. Although organic carbon concentrations are generally low, they are typical for pelagic sedimentary environments (e.g., Ziebis et al., 2012). Concentrations of OC, Fe_R , and Mn_R are generally higher in the finer grain sediments as compared to the coarser sedimentary horizons (Table T5).

Table T6 presents results for Fe, Mn, and Al from dithionite extractions on samples that were identified to be rich in volcanic ash/tephra. These sediments show that these layers can vary significantly in their Fe_R and Mn_R concentrations.

Acknowledgments

This report used samples and data provided by the Integrated Ocean Drilling Program (IODP). IODP is sponsored by the U.S. National Science Foundation (NSF). Financial support was provided by the U.S. Science Support Program (USSSP) and the US National Science Foundation under grant Number 1360077 for shore-based analyses.

References

- Expedition 340 Scientists, 2013a. Expedition 340 summary. *In* Le Friant, A., Ishizuka, O., Stroncik, N.A., and the Expedition 340 Scientists, *Proceedings of the Integrated Ocean Drilling Program*, 340: Tokyo (Integrated Ocean Drilling Program Management International, Inc.). <http://dx.doi.org/10.2204/iodp.proc.340.101.2013>
- Expedition 340 Scientists, 2013b. Methods. *In* Le Friant, A., Ishizuka, O., Stroncik, N.A., and the Expedition 340 Scientists, *Proceedings of the Integrated Ocean Drilling Pro-*



- gram, 340: Tokyo (Integrated Ocean Drilling Program Management International, Inc.). <http://dx.doi.org/10.2204/iodp.proc.340.102.2013>
- Goñi, M.A., Teixeira, M.J., and Perkey, D.W., 2003. Sources and distribution of organic matter in a river-dominated estuary (Winyah Bay, SC, USA). *Estuarine, Coastal and Shelf Science*, 57(5–6):1023–1048. [http://dx.doi.org/10.1016/S0272-7714\(03\)00008-8](http://dx.doi.org/10.1016/S0272-7714(03)00008-8)
- Hedges, J.I., and Stern, J.H., 1984. Carbon and nitrogen determinations of carbonate-containing solids. *Limnology and Oceanography*, 29(3):657–663. <http://dx.doi.org/10.4319/lo.1984.29.3.0657>
- Kostka, J.E., and Luther, G.W., III, 1994. Partitioning and speciation of solid phase iron in saltmarsh sediments. *Geochimica et Cosmochimica Acta*, 58(7):1701–1710. [http://dx.doi.org/10.1016/0016-7037\(94\)90531-2](http://dx.doi.org/10.1016/0016-7037(94)90531-2)
- Le Friant, A., Ishizuka, O., Boudon, G., Palmer, M.R., Talling, P.J., Villemant, B., Adachi, T., Aljahdali, M., Breitkreuz, C., Brunet, M., Caron, B., Coussens, M., Deplus, C., Endo, D., Feuillet, N., Fraas, A.J., Fujinawa, A., Hart, M.B., Hatfield, R.B., Hornbach, M., Jutzeler, M., Kataoka, K.S., Komorowski, J.-C., Lebas, E., Lafuerza, S., Maeno, F., Manga, M., Martínez-Colon, M., McCanta, M., Morgan, S., Saito, T., Slagle, A., Sparks, S., Stinton, A., Stroncik, N., Subramanyam, K.S.V., Tamura, Y., Trofimovs, J., Voight, B., Wall-Palmer, D., Wang, F., and Watt, S.F.L., 2015. Submarine record of volcanic island construction and collapse in the Lesser Antilles arc: first scientific drilling of submarine volcanic island landslides by IODP Expedition 340. *Geochemistry, Geophysics, Geosystems*, 16(2):420–442. <http://dx.doi.org/10.1002/2014GC005652>
- Manheim, F.T., 1966. A hydraulic squeezer for obtaining interstitial waters from consolidated and unconsolidated sediments. *U. S. Geological Survey Professional Paper*, 550-C:256–261.
- Mehra, O.P., and Jackson, M.L., 1960. Iron oxide removal from soils and clays by a dithionite-citrate system buffered with sodium bicarbonate. *Clays and Clay Minerals*, 7:317–327. <http://dx.doi.org/10.1346/CCMN.1958.0070122>
- Muratli, J.M., McManus, J., Mix, A., and Chase, Z., 2012. Dissolution of fluoride complexes following microwave-assisted hydrofluoric acid digestion of marine sediments. *Talanta*, 89:195–200. <http://dx.doi.org/10.1016/j.talanta.2011.11.081>
- Muratli, J.M., Megowan, M.R., and McManus, M., 2015. Data report: sediment major element, minor element, and reactive iron and manganese data from the Okinawa Trough: IODP Expedition 331 Sites C0014 and C0017. In Takai, K., Mottl, M.J., Nielsen, S.H., and the Expedition 331 Scientists, *Proceedings of the Integrated Ocean Drilling Program*, 331: Tokyo (Integrated Ocean Drilling Program Management International, Inc.). <http://dx.doi.org/10.2204/iodp.proc.331.202.2015>
- Palmer, M.R., Hatter, S.J., Gernon, T.M., Taylor, R.N., Cassidy, M., Johnson, P., Le Friant, A., and Ishiquka, O., 2016. Discovery of a large 2.4 Ma Plinian eruption of Basse-Terre, Guadeloupe, from the marine sediment record. *Geology*, 44(2):123–126. <http://dx.doi.org/10.1130/G37193.1>
- Roy, M., McManus, J., Goñi, M.A., Chase, Z., Borgeld, J.C., Wheatcroft, R.A., Muratli, J.M., Megowan, M.R., and Mix, A., 2013. Reactive iron and manganese distributions in seabed sediments near small mountainous rivers off Oregon and California (USA). *Continental Shelf Research*, 54:67–69. <http://dx.doi.org/10.1016/j.csr.2012.12.012>
- Ziebis, W., McManus, J., Ferdelman, T., Schmidt-Schierhorn, F., Bach, W., Muratli, J., Edwards, K.J., and Villinger, H., 2012. Interstitial fluid chemistry of sediments underlying the North Atlantic Gyre and the influence of subsurface fluid flow. *Earth and Planetary Science Letters*, 323–324:79–91. <http://dx.doi.org/10.1016/j.epsl.2012.01.018>

Initial receipt: 6 March 2016

Acceptance: 15 August 2016

Publication: 26 October 2016

MS 340-207



Figure F1. Map of study area, Expedition 340. Data from sites presented in this report are indicated by solid circles.

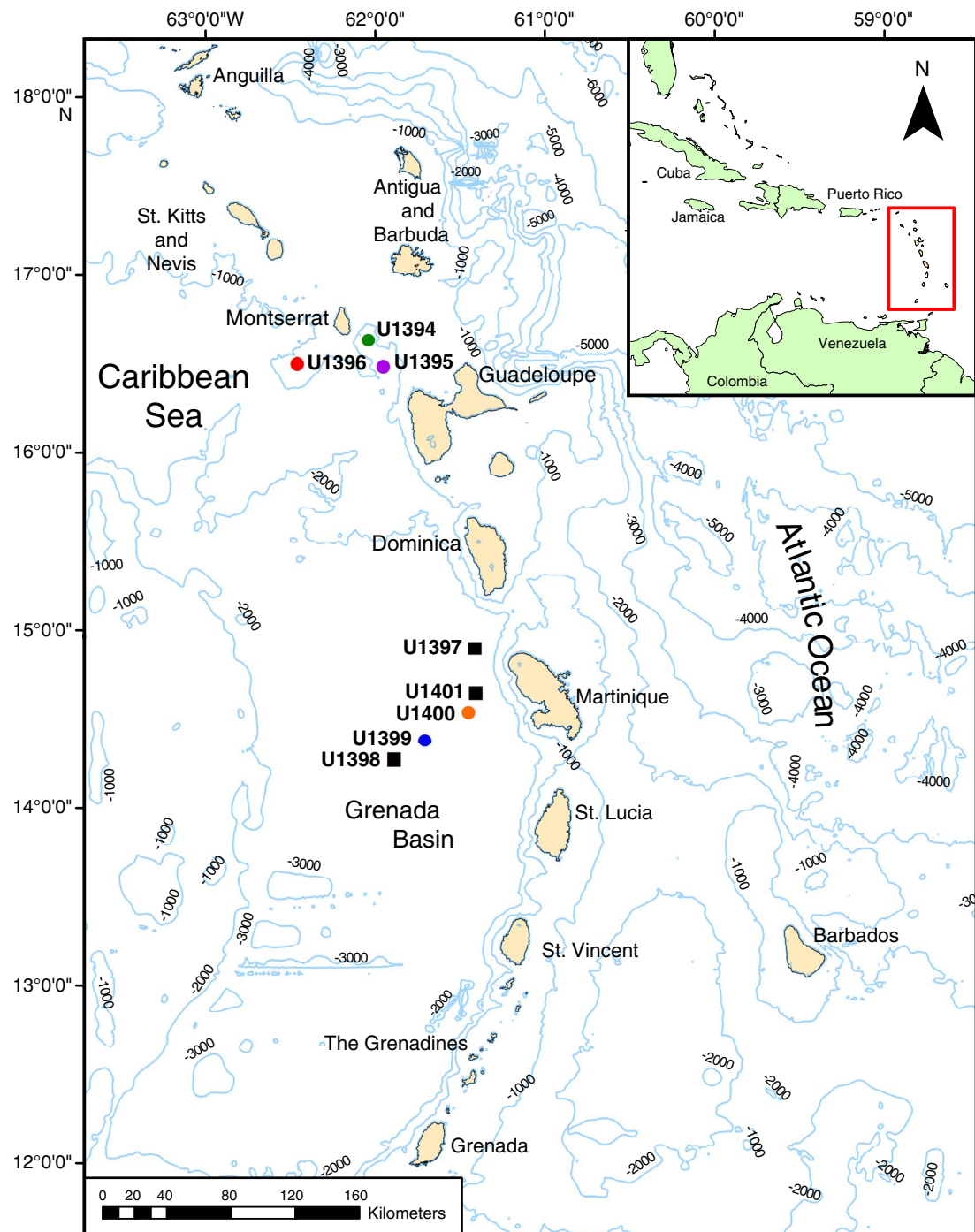


Figure F2. Dissolved pore fluid concentrations as a function of sediment depth, Hole U1394B. A. Ca and Mg. B. S and Mn. C. B and Si. D. Li and Sr. E. Cs and Rb. Dashed lines = bottom water concentrations.

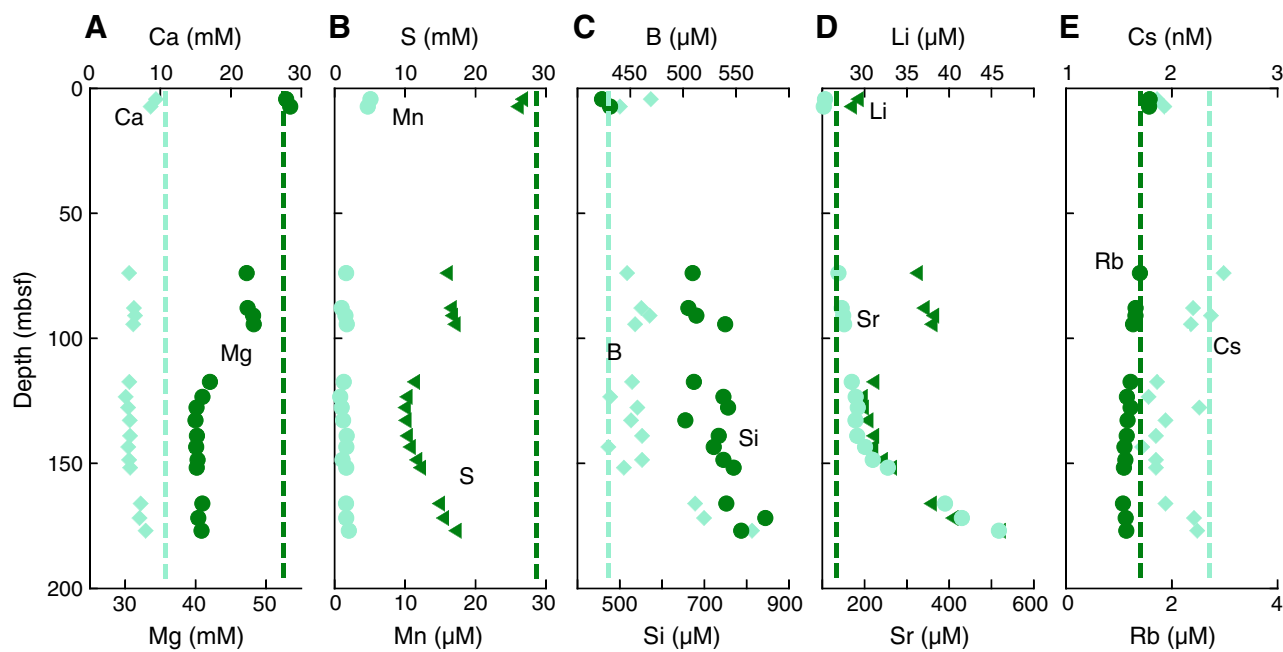


Figure F3. Dissolved pore fluid concentrations as a function of sediment depth, Hole U1395B. A. Ca and Mg. B. S and Mn. C. B and Si. D. Li and Sr. E. Cs and Rb. Dashed lines = bottom water concentrations.

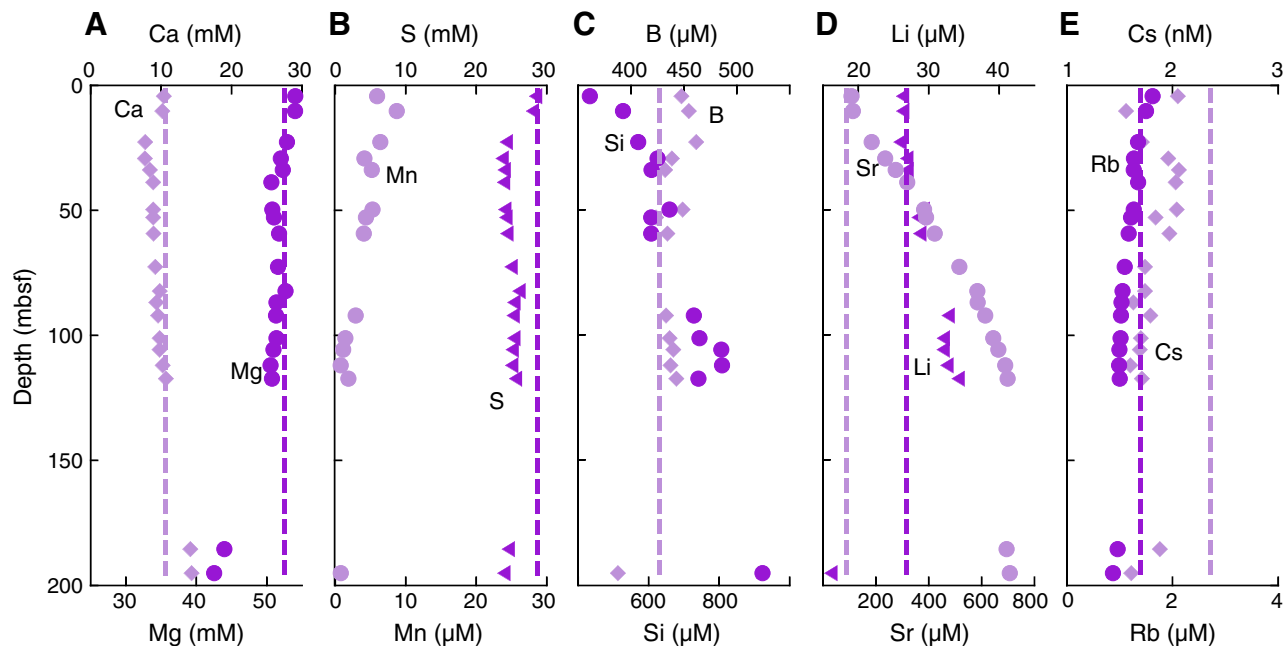


Figure F4. Dissolved pore fluid concentrations as a function of sediment depth, Hole U1396C. A. Ca and Mg. B. S and Mn. C. B and Si. D. Li and Sr. E. Cs and Rb. Dashed lines = bottom water concentrations.

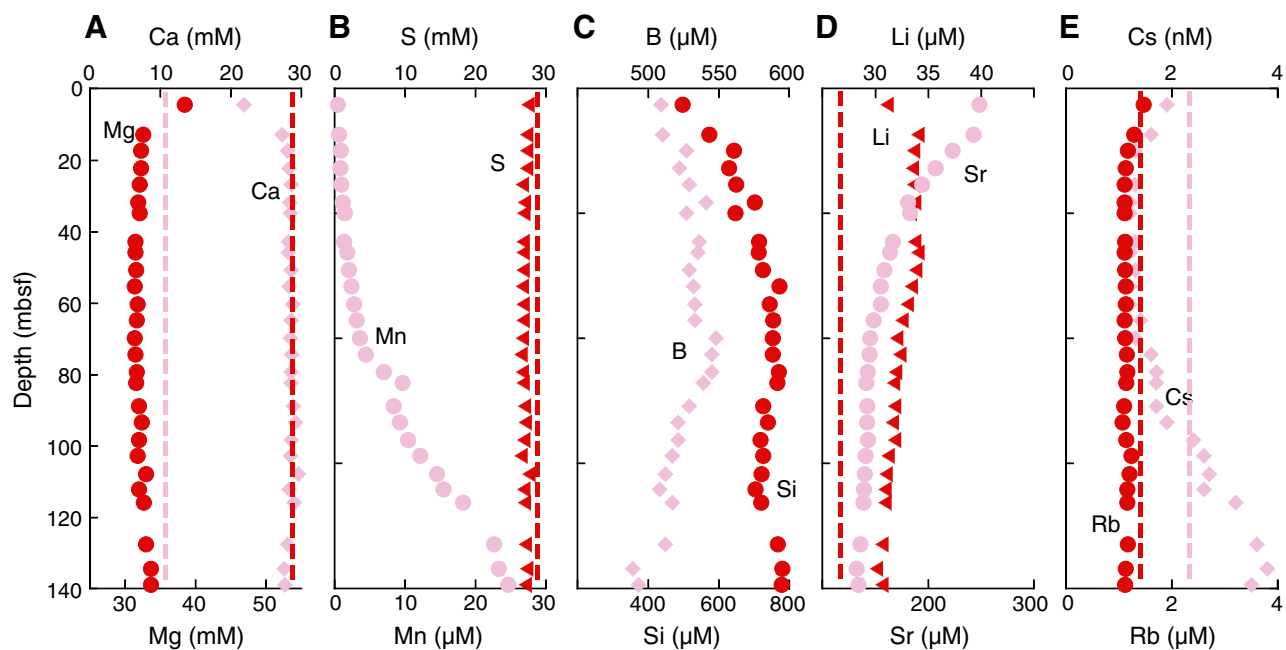


Figure F5. Dissolved pore fluid concentrations as a function of sediment depth, Hole U1399B. A. Ca and Mg. B. S and Mn. C. B and Si. D. Li and Sr. E. Cs and Rb. Dashed lines = bottom water concentrations.

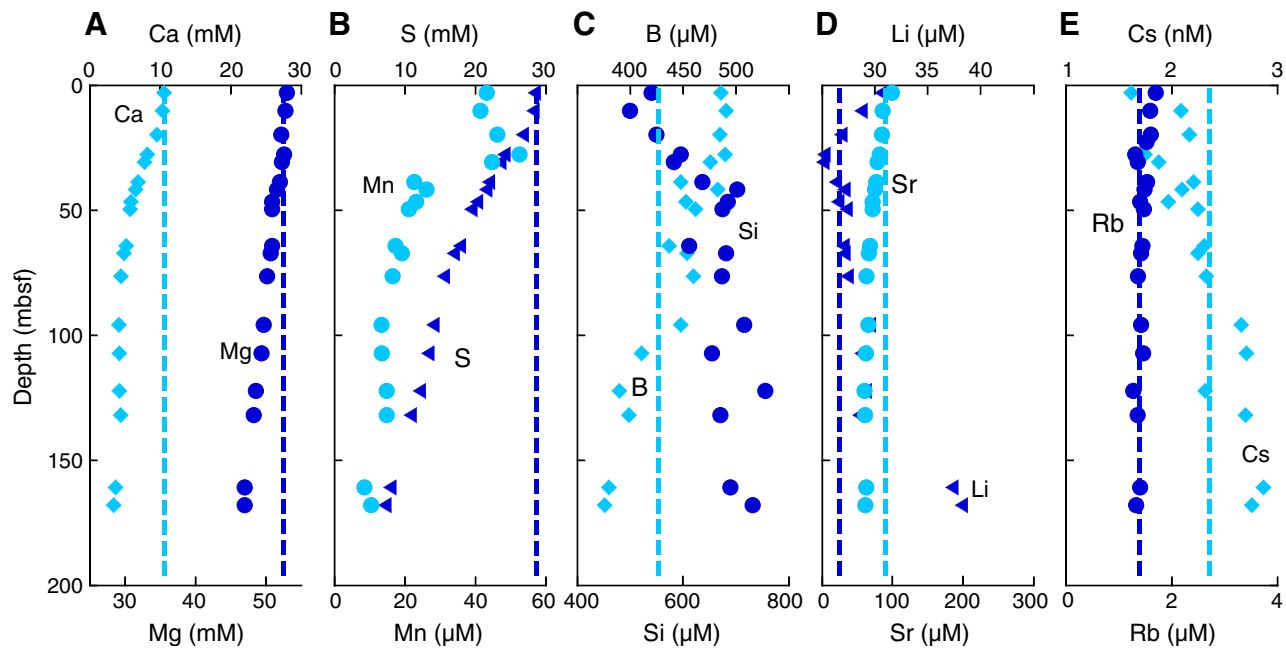


Figure F6. Dissolved pore fluid concentrations as a function of sediment depth, Holes U1400B and U1400C. A. Ca and Mg. B. S and Mn. C. B and Si. D. Li and Sr. E. Cs and Rb. Dashed lines = bottom water concentrations.

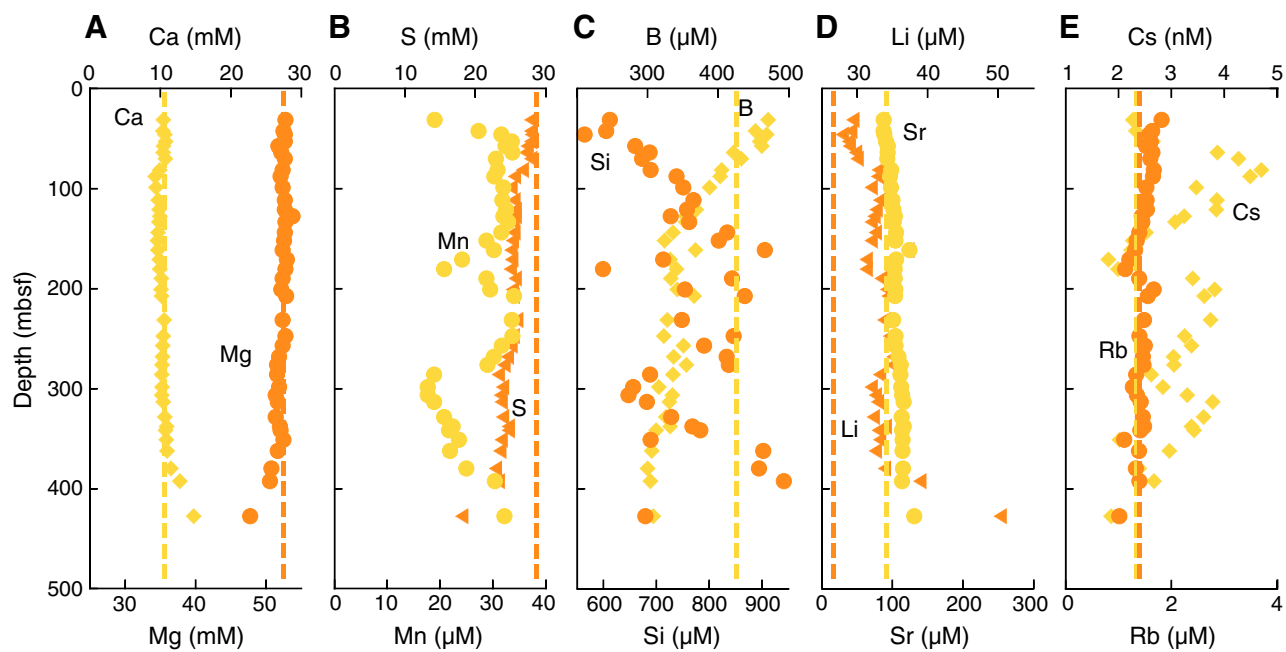


Figure F7. Solid-phase (A) Fe_R , (B) Mn_R , (C) organic carbon (OC), and (D) CaCO_3 vs. sediment depth, Hole U1394A.

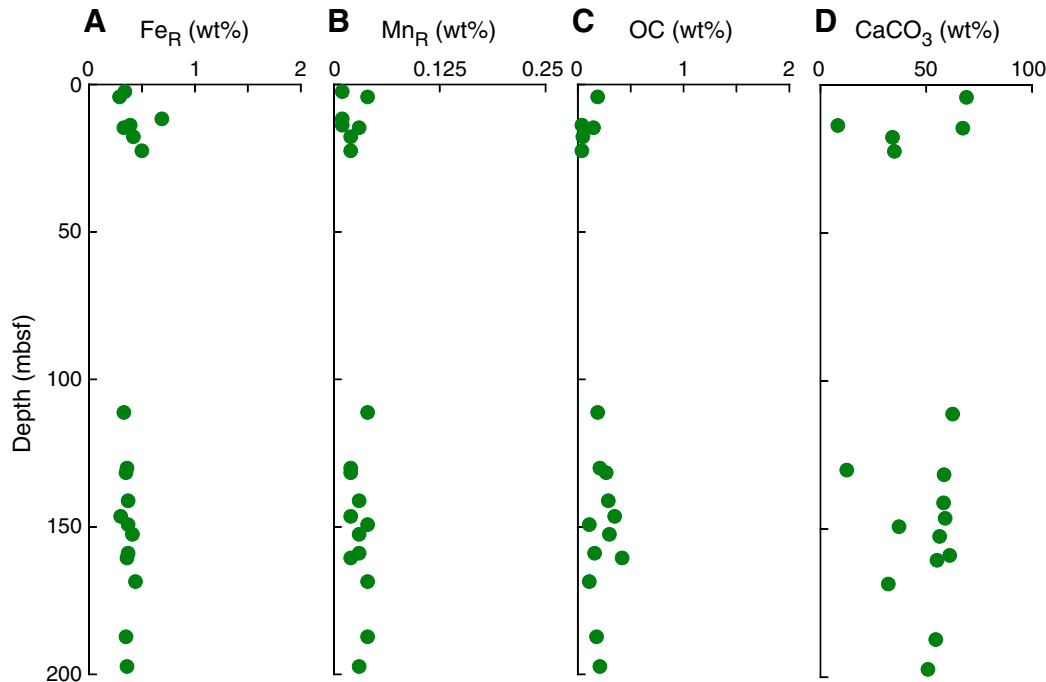


Figure F8. Solid-phase (A) Fe_R , (B) Mn_R , (C) organic carbon (OC), and (D) CaCO_3 vs. sediment depth, Hole U1395A.

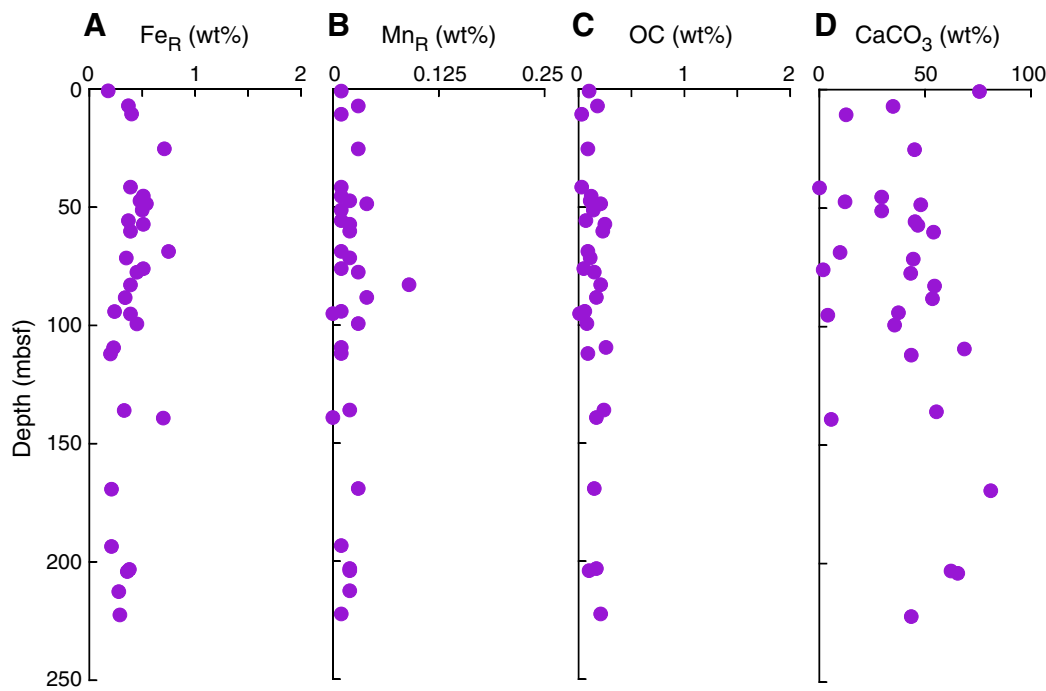


Figure F9. Solid-phase (A) Fe_R , (B) Mn_R , (C) organic carbon (OC), and (D) CaCO_3 vs. sediment depth, Hole U1396A.

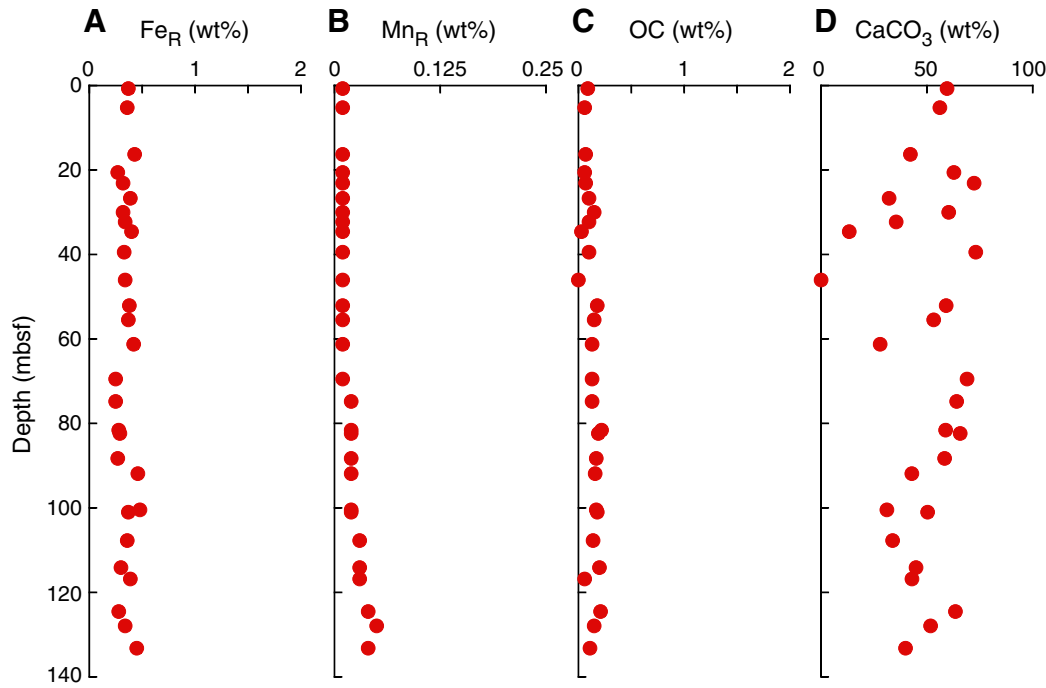


Figure F10. Solid-phase (A) Fe_R , (B) Mn_R , (C) organic carbon (OC), and (D) CaCO_3 vs. sediment depth, Hole U1399A.

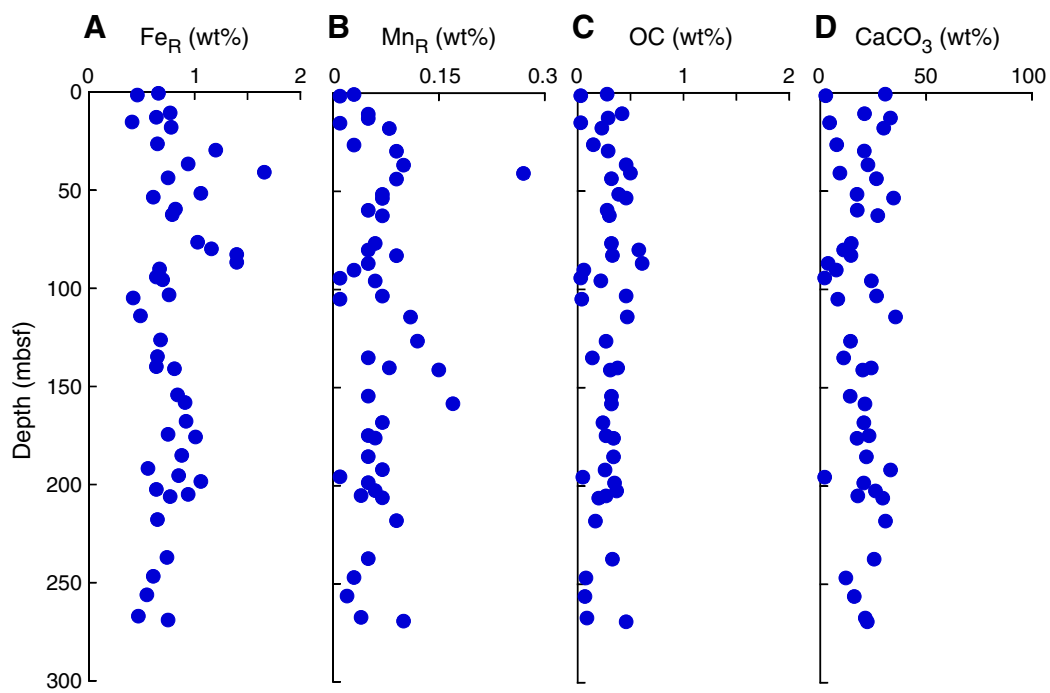


Figure F11. Solid-phase (A) Fe_R , (B) Mn_R , (C) organic carbon (OC), and (D) CaCO_3 vs. sediment depth, Holes U1400B and U1400C.

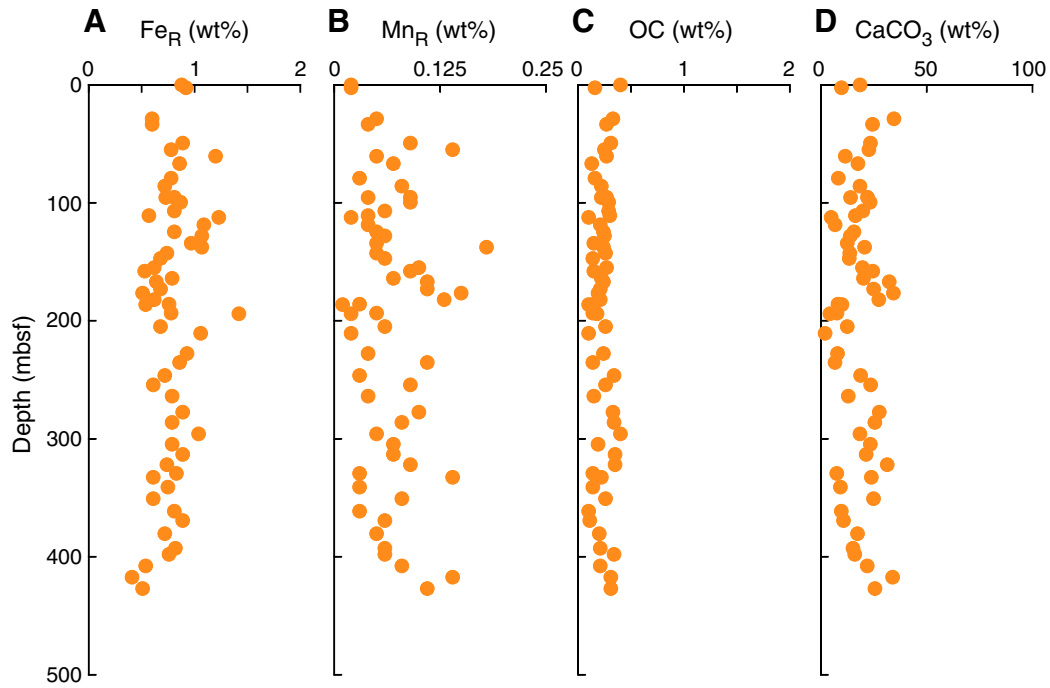


Figure F12. Solid-phase (A) Fe_R , (B) Mn_R , (C) organic carbon (OC), and (D) CaCO_3 vs. sediment depth, Section 340-U1399B-3H-3. Core photo retrieved from on-board data archive (<http://web.iodp.tamu.edu/LORE/>).

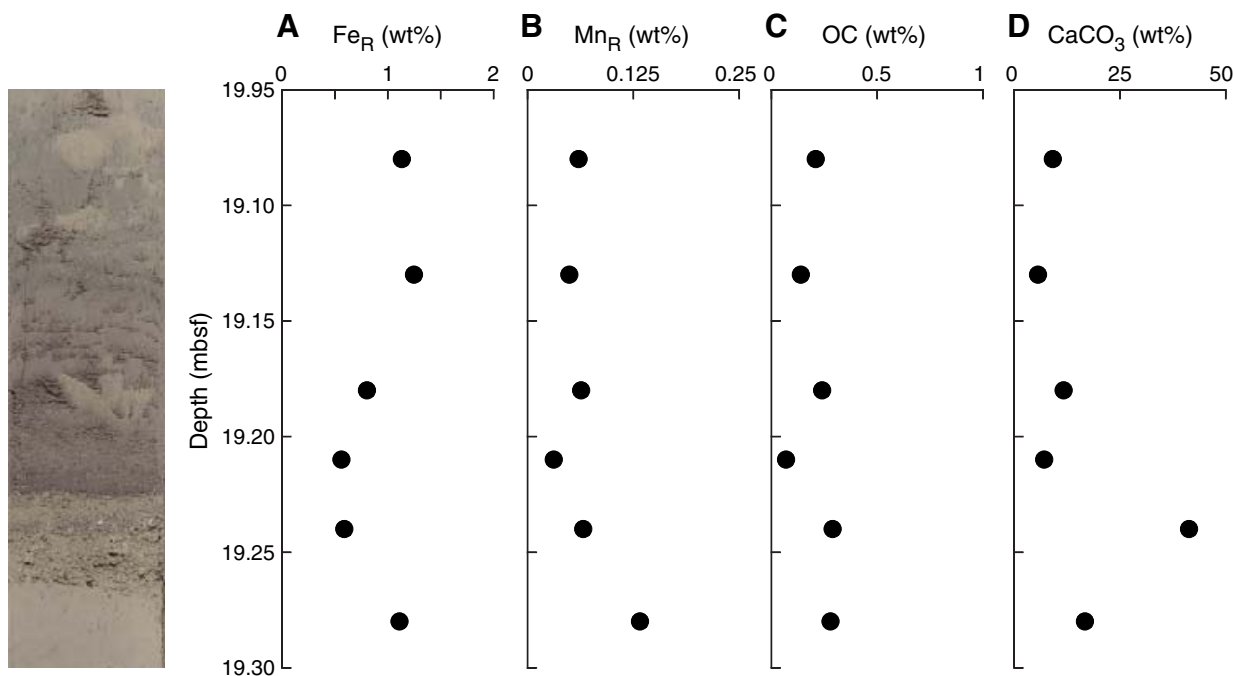


Figure F13. Solid-phase (A) Fe_R , (B) Mn_R , (C) organic carbon (OC), and (D) CaCO_3 vs. sediment depth, Section 340-U1399B-7H-3. Core photo retrieved from onboard data archive (<http://web.iodp.tamu.edu/LORE/>).

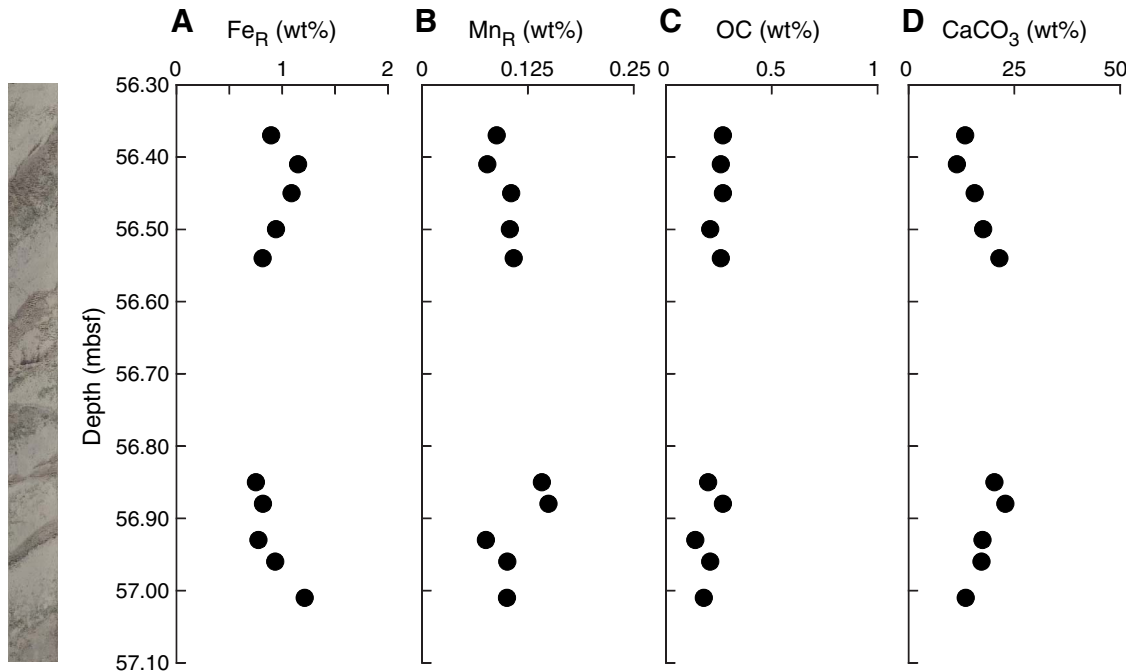


Figure F14. Solid-phase (A) Fe_R , (B) Mn_R , (C) organic carbon (OC), and (D) CaCO_3 vs. sediment depth, Section 340-U1399B-11H-2. Core photo retrieved from onboard data archive (<http://web.iodp.tamu.edu/LORE/>).

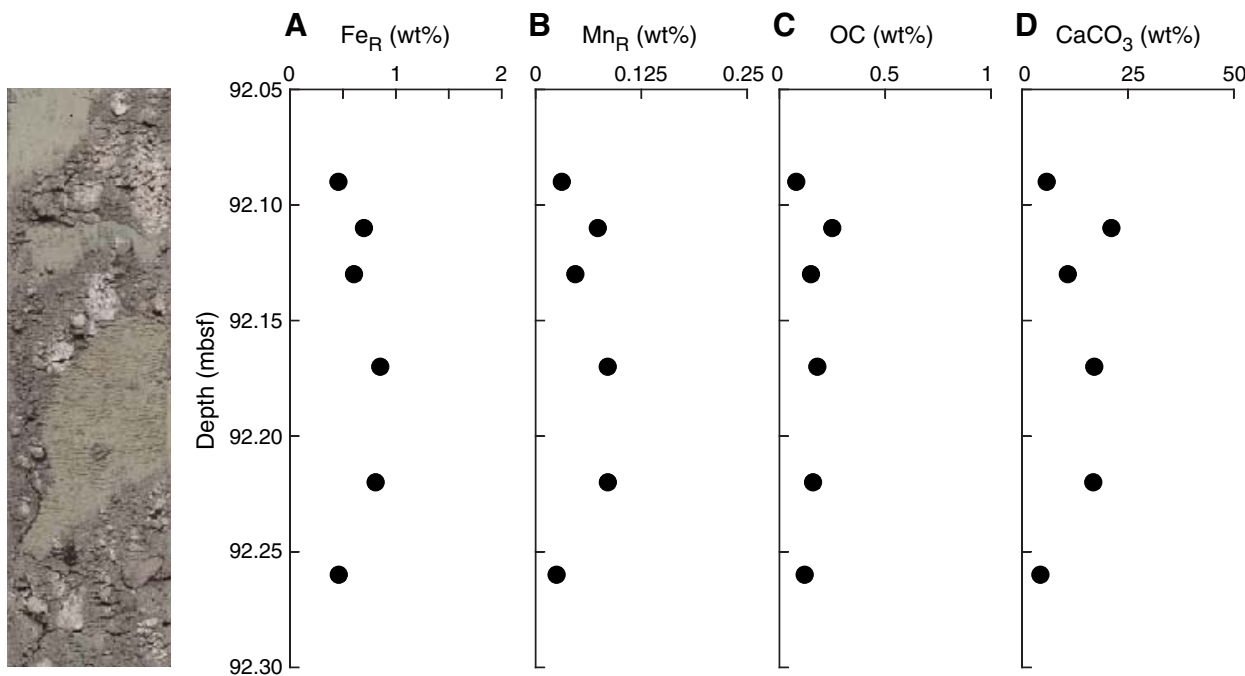


Figure F15. Solid-phase (A) Fe_R , (B) Mn_R , (C) organic carbon (OC), and (D) CaCO_3 vs. sediment depth, Section 340-U1399B-16H-2. Core photo retrieved from onboard data archive (<http://web.iodp.tamu.edu/LORE/>).

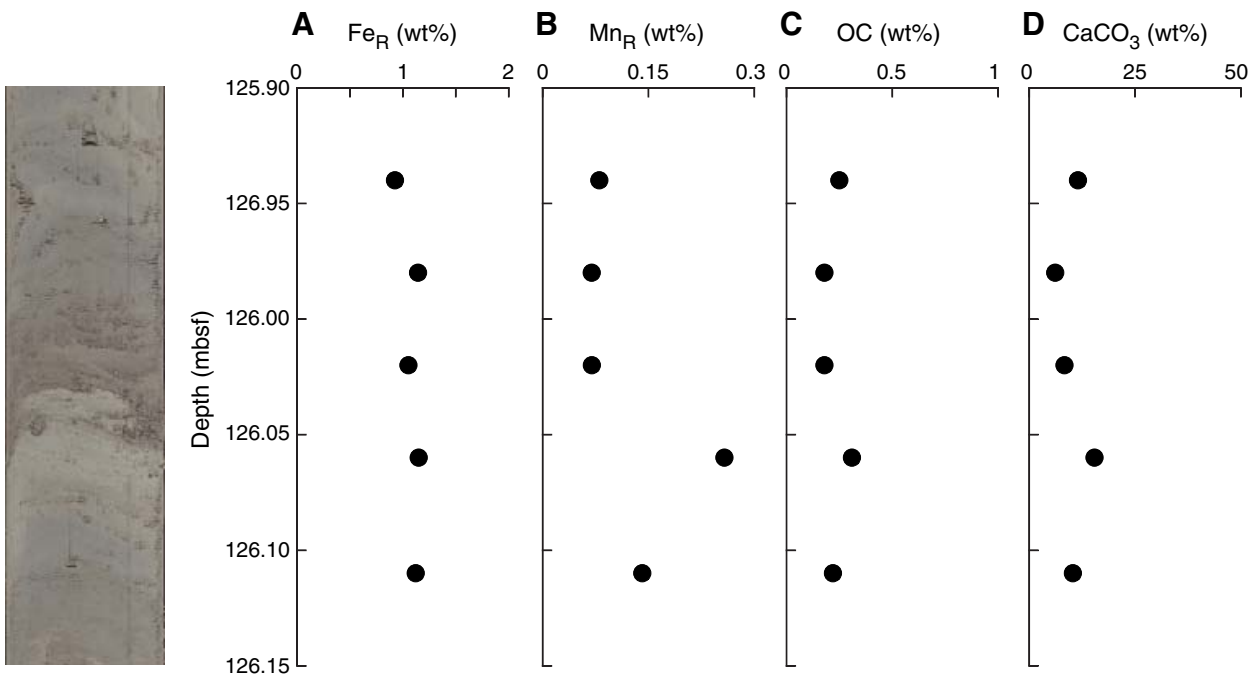


Figure F16. Solid-phase (A) Fe_R , (B) Mn_R , (C) organic carbon (OC), and (D) CaCO_3 vs. sediment depth, Section 340-U1399B-19H-2. Core photo retrieved from onboard data archive (<http://web.iodp.tamu.edu/LORE/>).

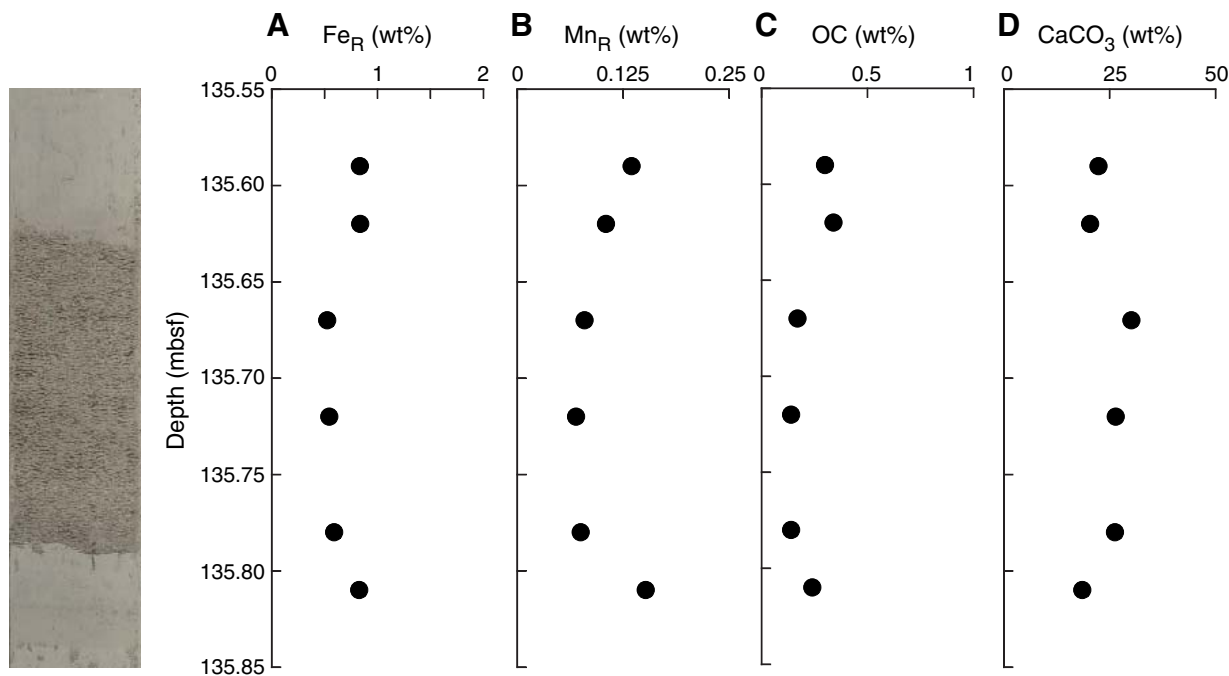


Figure F17. Solid-phase (A) Fe_R , (B) Mn_R , (C) organic carbon (OC), and (D) CaCO_3 vs. sediment depth, Section 340-U1399B-25H-2. Core photo retrieved from onboard data archive (<http://web.iodp.tamu.edu/LORE/>).

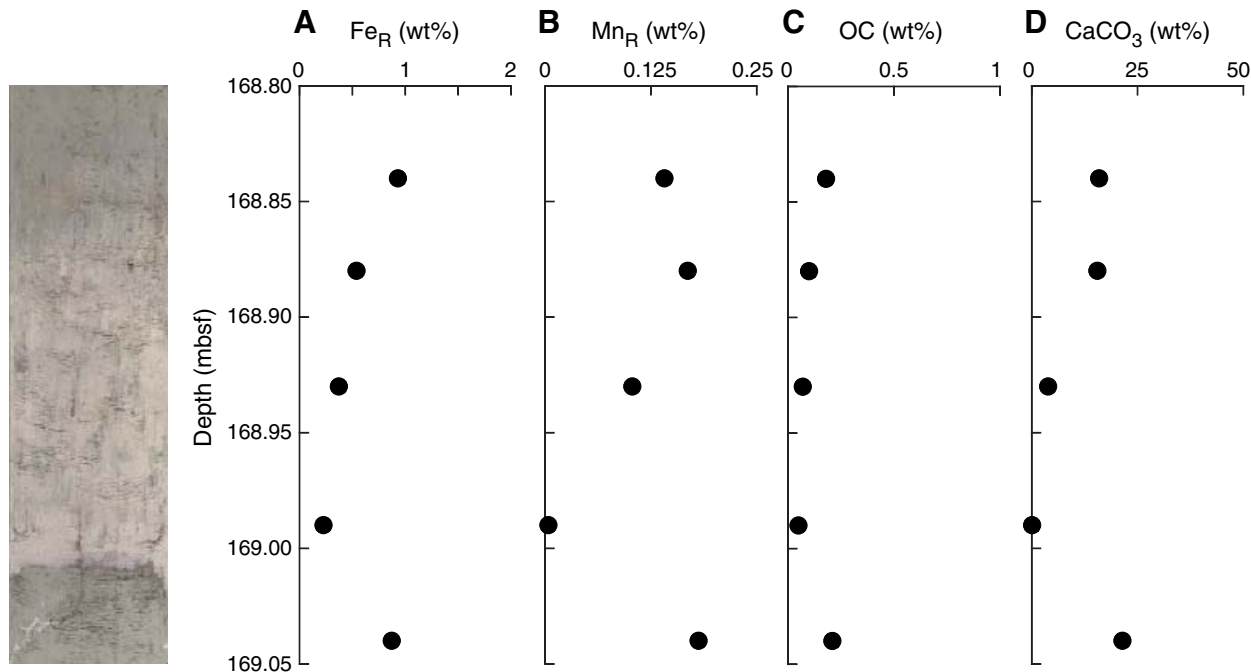


Figure F18. Solid-phase (A) Fe_R , (B) Mn_R , (C) organic carbon (OC), and (D) CaCO_3 vs. sediment depth, Section 340-U1400B-16H-2. Core photo retrieved from onboard data archive (<http://web.iodp.tamu.edu/LORE/>).

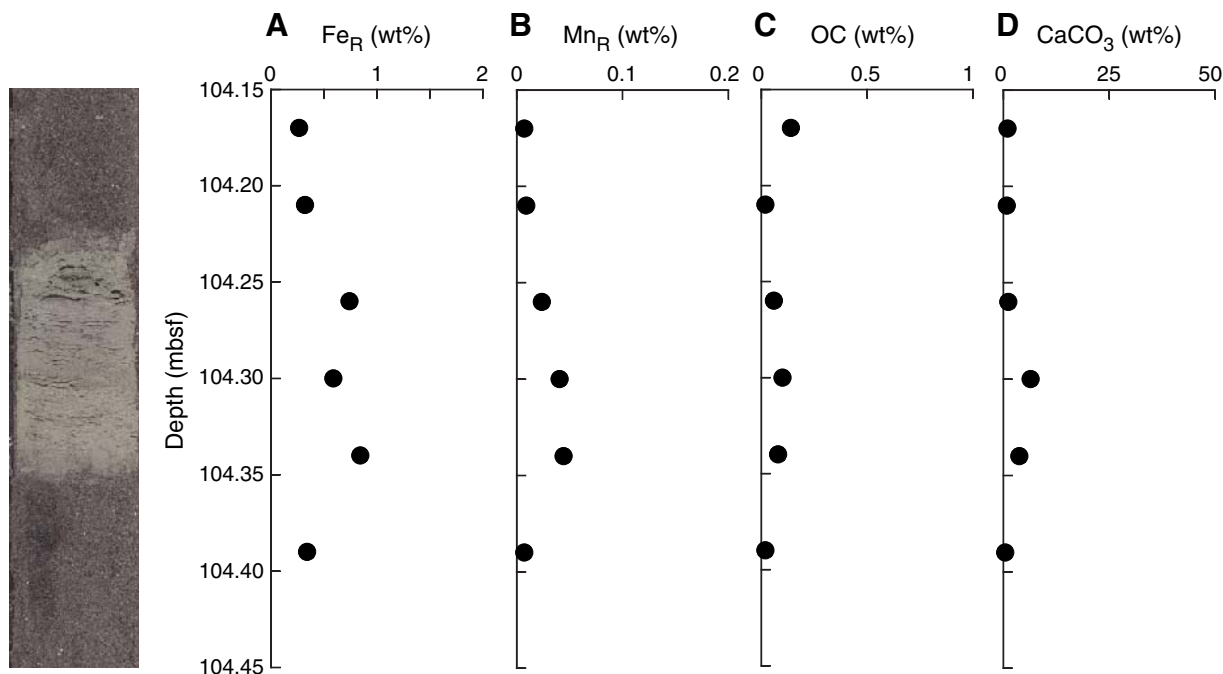


Figure F19. Solid-phase (A) Fe_R , (B) Mn_R , (C) organic carbon (OC), and (D) CaCO_3 vs. sediment depth, Section 340-U1400B-26H-5. Core photo retrieved from onboard data archive (<http://web.iodp.tamu.edu/LORE/>).

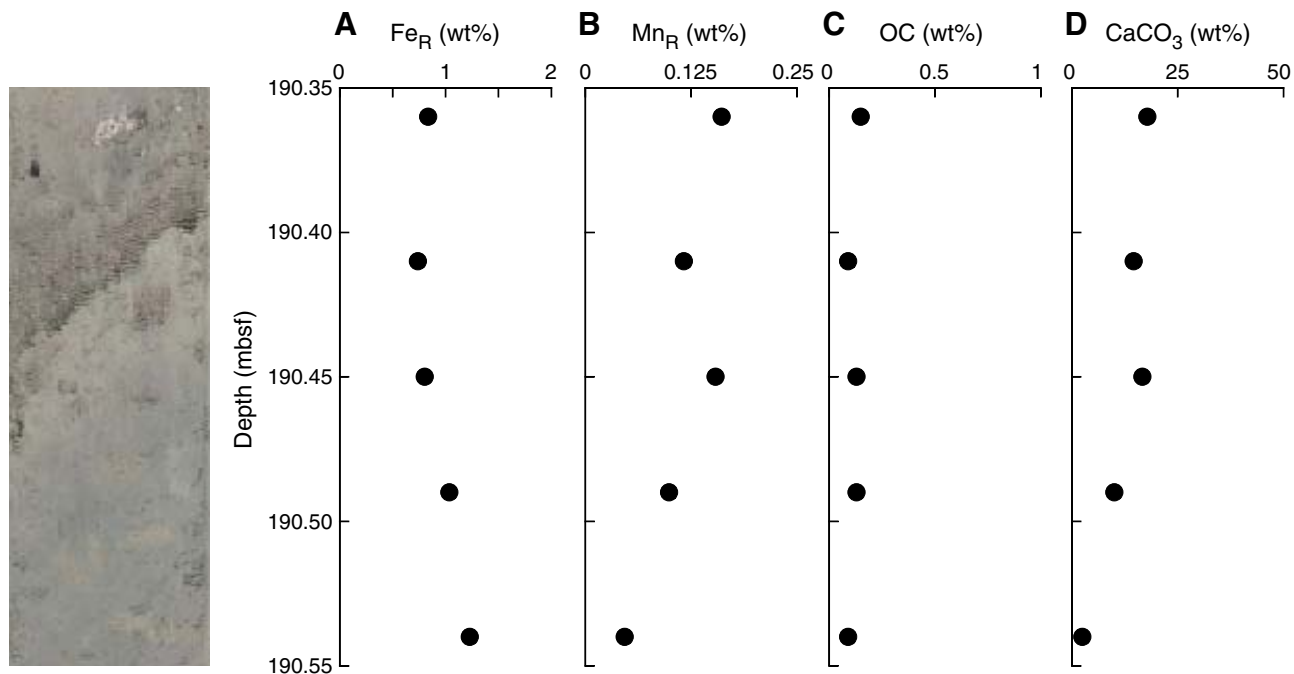


Figure F20. Solid-phase (A) Fe_R , (B) Mn_R , (C) organic carbon (OC), and (D) CaCO_3 vs. sediment depth, Section 340-U1400C-48X-1. Core photo retrieved from onboard data archive (<http://web.iodp.tamu.edu/LORE/>).

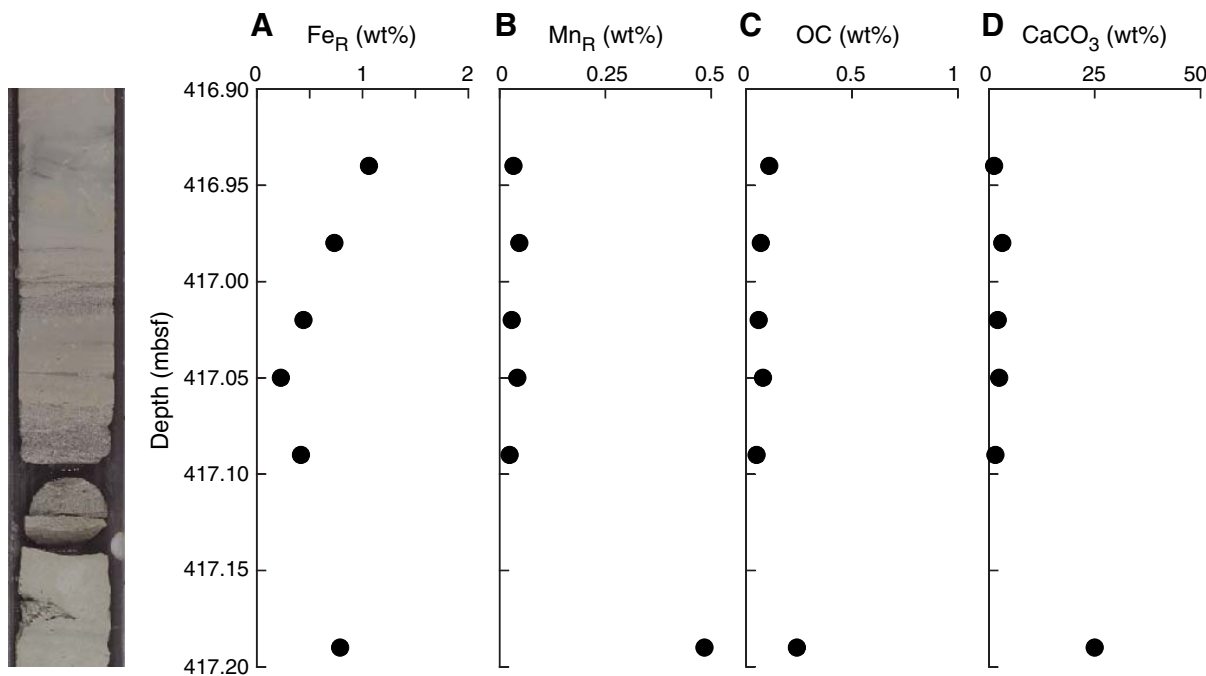


Table T1. Pore fluid composition, Holes U1394B, U1395B, U1396C, U1399B, U1400B, and U1400C. (Continued on next page.)

Core, section	Depth CSF-A (m)		Li (µM)	± (µM)	B (µM)	± (µM)	Si (µM)	± (µM)	Mn (µM)	± (µM)	Sr (µM)	± (µM)	Rb (µM)	± (µM)	Cs (pM)	± (pM)
	Top	Bottom														
340-U1394B-																
1H-3	4.40	4.45	29.1	0.6	469	3	458	3	5.08	0.04	106	1	1.58	0.02	1.9	0.2
1H-5	7.30	7.35	28.3	0.7	440	5	477	5	4.71	0.06	103	1	1.57	0.02	1.9	0.1
10H-1	73.90	73.95	36.1	0.6	447	1	672	3	1.63	0.04	138	1	1.40	0.01	2.5	0.2
11H-4	87.92	88.02	36.9	0.6	460	3	662	6	0.99	0.04	146	1	1.31	0.02	2.2	0.1
11H-6	90.92	91.02	38.1	0.6	468	2	681	7	1.54	0.04	149	1	1.31	0.02	2.4	0.2
12H-2	94.40	94.50	37.8	0.6	455	2	749	3	1.72	0.04	152	1	1.27	0.01	2.2	0.1
14H-5	117.40	117.50	31.0	0.6	452	4	675	5	1.30	0.04	170	1	1.22	0.02	1.9	0.1
15H-3	123.40	123.50	29.6	0.6	431	3	745	3	0.79	0.04	179	1	1.15	0.01	1.8	0.1
15H-6	127.72	127.82	29.7	0.6	457	2	756	5	1.01	0.04	184	1	1.22	0.02	2.3	0.1
16H-3	132.80	132.90	30.3	0.6	451	1	655	4	1.20	0.04	178	1	1.16	0.02	1.9	0.1
17H-3	139.00	139.10	30.9	0.6	461	4	734	5	1.70	0.06	183	1	1.15	0.01	1.9	0.2
17H-6	143.46	143.56	30.8	0.3	429	1	722	3	1.66	0.07	201	5	1.11	0.02	1.7	0.1
18H-3	148.60	148.70	32.0	0.6	461	2	745	5	1.12	0.04	219	5	1.12	0.01	1.8	0.1
18H-6	151.72	151.82	33.1	0.6	444	6	769	5	1.65	0.04	255	5	1.09	0.01	1.8	0.1
20H-2	166.10	166.20	37.8	0.6	511	3	752	3	1.62	0.05	390	5	1.08	0.01	1.9	0.2
20H-6	171.87	171.97	40.3	0.3	520	0	844	2	1.64	0.05	430	5	1.13	0.01	2.2	0.1
21H-3	176.93	177.03	45.9	0.6	565	2	787	5	2.02	0.04	517	5	1.14	0.02	2.2	0.1
340-U1395B-																
1H-3	4.40	4.50	26.3	0.6	448	1	433	3	5.93	0.04	108	1	1.62	0.03	2.0	0.2
2H-3	10.30	10.40	26.3	0.6	455	3	527	3	8.72	0.08	113	1	1.50	0.01	1.6	0.1
3H-5	22.70	22.80	25.9	0.6	462	1	570	3	6.39	0.05	184	1	1.35	0.01	1.7	0.2
4H-3	29.32	29.42	26.9	0.6	439	2	625	4	4.13	0.04	235	5	1.27	0.02	2.0	0.1
4H-6	33.88	33.98	26.9	0.6	432	3	608	3	5.18	0.05	275	5	1.26	0.02	2.1	0.1
5H-3	38.80	38.90									318	5	1.35	0.02	2.0	0.1
6H-4	49.72	49.82	29.2	0.6	449	2	659	3	5.28	0.04	382	5	1.27	0.02	2.0	0.2
6H-6	52.85	52.95	28.5	0.6	424	3	607	3	4.35	0.05	390	6	1.21	0.01	1.8	0.1
7H-4	59.31	59.41	28.7	0.6	434	4	607	3	4.04	0.04	422	6	1.17	0.02	2.0	0.2
9H-1	72.60	72.70									516	5	1.10	0.01	1.7	0.1
10H-2	82.30	82.40									584	5	1.05	0.02	1.7	0.1
10H-5	86.81	86.91									585	6	1.03	0.02	1.6	0.2
11H-3	92.10	92.20	32.8	0.6	433	2	728	5	2.88	0.04	614	6	1.03	0.01	1.8	0.1
12H-3	101.15	101.25	32.1	0.6	436	1	744	4	1.43	0.04	644	6	1.02	0.01	1.7	0.1
12H-6	105.70	105.80	32.0	0.6	440	3	806	3	1.11	0.04	663	5	0.99	0.02	1.7	0.1
13H-4	112.02	112.12	32.6	0.6	437	4	808	3	0.77	0.04	689	5	0.99	0.01	1.6	0.2
14H-3	117.30	117.40	34.2	0.6	443	3	741	4	1.85	0.04	698	7	1.00	0.02	1.7	0.2
24X-1	185.50	185.60									694	7	0.96	0.02	1.9	0.1
25X-1	195.10	195.20	16.1	0.6	388	1	923	5	0.78	0.04	706	5	0.87	0.01	1.6	0.1
340-U1396C-																
1H-3	4.40	4.50	31.1	0.6	509	1	497	3	0.40	0.04	248.2	5	1.46	0.01	1.9	0.1
2H-3	12.80	12.90	34.0	0.6	510	3	573	3	0.56	0.05	242.7	5	1.28	0.02	1.6	0.1
2H-6	17.30	17.40	33.6	0.6	527	2	643	5	0.83	0.05	222.9	5	1.16	0.01	1.3	0.1
3H-3	22.20	22.30	33.5	0.6	522	3	629	3	0.77	0.04	206.7	5	1.12	0.02	1.1	0.1
3H-6	26.80	26.90	33.6	0.6	529	4	649	5	0.90	0.04	194.0	5	1.10	0.02	1.3	0.1
4H-3	31.80	31.90	33.7	0.6	541	5	702	3	1.08	0.04	181	1	1.10	0.01	1.2	0.1
4H-5	34.80	34.90	33.3	0.6	527	1	647	4	1.38	0.04	183	1	1.10	0.01	1.2	0.1
5H-4	42.80	42.90	33.7	0.6	536	2	714	4	1.29	0.04	166	2	1.11	0.02	1.3	0.2
5H-6	45.80	45.90	34.0	0.6	535	3	713	5	1.74	0.04	164	1	1.10	0.01	1.2	0.2
6H-3	50.70	50.80	33.8	0.6	529	3	725	3	1.96	0.05	158	1	1.11	0.02	1.3	0.1
6H-6	55.30	55.40	33.4	0.6	532	2	772	4	2.32	0.04	155	2	1.12	0.01	1.2	0.1
7H-3	60.30	60.40	33.0	0.6	533	6	744	6	2.71	0.05	155	1	1.12	0.02	1.2	0.1
7H-6	64.80	64.90	32.5	0.6	533	4	754	4	3.08	0.05	148	1	1.10	0.01	1.4	0.1
8H-3	69.80	69.90	32.0	0.6	548	3	753	4	3.54	0.05	145	1	1.11	0.02	1.3	0.2
8H-6	74.35	74.45	32.3	0.6	545	2	753	3	4.39	0.04	144	1	1.14	0.01	1.6	0.1
9H-3	79.30	79.40	31.9	0.6	545	4	770	4	6.92	0.05	143	1	1.15	0.02	1.7	0.1
9H-5	82.30	82.40	31.7	0.6	539	4	766	4	9.59	0.11	141	1	1.13	0.02	1.7	0.1
10H-3	88.82	88.92	31.8	0.6	529	3	726	3	8.32	0.05	142	1	1.09	0.02	1.7	0.2
10H-6	93.35	93.45	31.6	0.6	521	3	739	3	9.20	0.06	142	1	1.06	0.01	1.9	0.2
11H-3	98.30	98.40	31.8	0.6	521	5	718	3	10.37	0.05	143	1	1.13	0.02	2.4	0.1
11H-6	102.71	102.81	31.2	0.6	517	2	726	4	12.10	0.08	141	1	1.23	0.02	2.6	0.2
12H-3	107.83	107.93	31.0	0.6	512	3	721	4	14.48	0.08	140	1	1.19	0.02	2.7	0.1
12H-6	112.10	112.20	30.9	0.6	508	3	704	3	15.40	0.05	139	1	1.15	0.01	2.6	0.1
13H-2	115.81	115.91	30.9	0.6	517	4	720	2	18.17	0.07	139	1	1.15	0.02	3.2	0.2
14H-5	127.49	127.59	30.6	0.6	512	3	767	3	22.57	0.10	136	1	1.16	0.01	3.6	0.2
15H-3	134.33	134.43	30.1	0.6	489	2	780	3	23.23	0.06	132	1	1.12	0.02	3.8	0.2
15H-6	138.80	138.90	30.6	0.6	493	1	778	4	24.58	0.18	134	1	1.11	0.01	3.5	0.2

Table T1 (continued).

Core, section	Depth CSF-A (m)		Li (μM)	\pm (μM)	B (μM)	\pm (μM)	Si (μM)	\pm (μM)	Mn (μM)	\pm (μM)	Sr (μM)	\pm (μM)	Rb (μM)	\pm (μM)	Cs (pM)	\pm (pM)
	Top	Bottom														
340-U1399B-																
1H-2	2.90	3.00	30.6	1.3	486	2	541	6	43.3	0.2	99	1	1.70	0.04	1.62	0.19
2H-3	10.10	10.20	28.7	1.3	491	3	500	6	41.5	0.3	86	1	1.60	0.02	2.09	0.13
3H-3	19.62	19.72	26.8	1.3	485	5	550	7	46.3	0.3	85	1	1.61	0.01	2.17	0.13
3H-5	22.60	22.70														
4H-2	27.60	27.70	25.2	1.3	490	2	596	6	52.6	0.2	82	1	1.32	0.01	1.75	0.13
4H-4	30.60	30.70	25.1	1.3	476	1	583	7	44.8	0.3	79	1	1.36	0.02	1.88	0.12
5H-3	38.60	38.70	26.3	1.3	448	3	637	6	22.7	0.1	77	1	1.54	0.02	2.21	0.12
5H-5	41.60	41.70	27.1	1.3	483	3	703	5	26.2	0.1	75	1	1.49	0.03	2.10	0.14
6H-2	46.50	46.60	26.5	1.3	453	5	685	7	23.3	0.1	72	1	1.41	0.01	1.97	0.12
6H-4	49.45	49.55	27.3	1.2	462	2	675	5	21.2	0.1	72	1	1.48	0.02	2.25	0.13
8H-1	64.12	64.22	27.0	1.3	437	3	612	5	17.4	0.1	68	1	1.45	0.02	2.31	0.14
8H-3	67.07	67.17	27.1	1.2	454	1	682	6	19.2	0.1	67	1	1.43	0.03	2.25	0.14
9H-3	76.32	76.42	27.4	1.3	460	3	674	6	16.6	0.1	63	1	1.37	0.02	2.33	0.17
12H-1	95.72	95.82	29.5	1.3	448	3	716	5	13.4	0.1	66	1	1.43	0.02	2.66	0.19
13H-3	107.10	107.20	28.7	1.3	411	2	655	6	13.5	0.1	62	1	1.47	0.02	2.71	0.18
15H-5	122.13	122.24	29.1	1.2	390	3	756	5	14.9	0.1	61	1	1.28	0.02	2.32	0.14
18H-2	131.83	131.93	28.5	1.2	399	2	671	6	14.9	0.1	61	1	1.36	0.02	2.70	0.15
24H-1	160.70	160.80	37.3	1.2	380	3	690	6	8.6	0.1	63	1	1.41	0.02	2.87	0.13
25H-1	167.80	167.90	38.2	1.3	376	3	732	5	10.5	0.1	62	1	1.33	0.01	2.76	0.12
340-U1400B-																
7H-4	31.24	31.34	29.4	1.3	471	5	612	7	19.0	0.1	88	1	1.81	0.06	2.27	0.15
8H-5	42.40	42.50	29.1	1.3	453	2	605	7	27.3	0.1	88	1	1.64	0.02	2.33	0.15
9H-1	45.90	46.00	27.9	1.3	469	4	564	6	31.6	0.2	89	1	1.58	0.02	2.57	0.15
10H-3	52.91	53.01	28.8	1.3	459	6	549	7	33.6	0.2	91	1	1.61	0.01	2.65	0.13
10H-6	57.42	57.52	28.9	1.3	462	4	660	6	32.4	0.2	93	1	1.52	0.02	2.52	0.12
11H-4	63.92	64.02	29.8	1.2	422	3	687	7	33.7	0.1	93	1	1.64	0.02	3.87	0.12
12H-2	70.08	70.18	30.0	1.2	433	4	673	6	30.6	0.1	93	1	1.60	0.01	4.27	0.13
13H-5	81.40	81.50	33.0	1.3	405	2	689	6	30.9	0.1	98	1	1.67	0.02	4.70	0.12
14H-3	87.85	87.95	32.9	1.2	403	2	738	6	30.3	0.1	97	1	1.65	0.02	4.49	0.17
15H-4	98.80	98.90	32.0	1.3	388	3	751	7	32.0	0.3	98	1	1.53	0.02	3.47	0.13
17H-4	111.53	111.63	33.2	1.2	365	3	770	6	31.8	0.2	100	1	1.53	0.02	3.86	0.19
18H-4	121.00	121.10	32.7	1.3	369	2	758	6	32.5	0.1	101	1	1.54	0.02	3.85	0.16
19H-2	127.52	127.62	32.4	1.2	354	3	727	5	32.0	0.1	103	1	1.44	0.02	3.24	0.14
20H-3	133.21	133.31	32.0	1.3	354	2	762	6	32.9	0.2	102	1	1.45	0.01	3.07	0.13
21H-5	143.82	143.92	32.6	1.2	336	2	834	6	31.6	0.1	105	1	1.39	0.01	2.52	0.12
22H-4	151.83	151.93	32.0	1.3	324	2	818	8	28.8	0.1	104	1	1.34	0.01	2.27	0.12
23H-4	161.35	161.45	37.2	1.2	368	3	905	10	30.2	0.3	124	1	1.32	0.02	2.24	0.15
24H-4	170.88	170.98	31.3	1.3	332	3	713	6	24.2	0.2	105	1	1.20	0.01	1.81	0.12
25H-4	180.34	180.44	31.3	1.2	341	1	599	6	20.8	0.1	103	1	1.13	0.01	1.99	0.12
26H-4	189.78	189.88	33.4	1.3	333	2	843	6	28.8	0.2	103	1	1.39	0.02	3.40	0.16
27H-5	200.79	200.89	34.2	1.2	342	2	754	6	29.5	0.1	104	1	1.66	0.03	3.82	0.13
28H-3	207.30	207.40	34.4	1.3	366	4	867	9	34.0	0.2	104	1	1.56	0.02	3.62	0.15
340-U1400C-																
27X-4	231.20	231.30	33.8	1.2	328	2	748	6	33.6	0.1	101	1	1.48	0.01	3.74	0.11
29X-2	247.40	247.50	34.6	1.3	323	2	846	6	33.7	0.3	104	1	1.39	0.02	3.25	0.19
30X-2	257.00	257.10	35.3	1.3	351	2	790	6	31.7	0.1	104	1	1.49	0.02	3.38	0.12
31X-3	268.10	268.20	35.1	1.3	337	2	833	9	30.2	0.2	109	1	1.46	0.01	3.04	0.13
32X-2	276.20	276.30	35.0	1.3	355	4	837	11	29.0	0.2	112	1	1.47	0.02	3.05	0.13
33X-2	285.80	285.90	33.2	1.3	336	2	688	6	18.9	0.1	111	1	1.33	0.01	2.62	0.16
35X-4	298.40	298.50	32.0	1.3	316	1	656	6	17.7	0.1	112	1	1.27	0.02	2.84	0.13
36X-3	306.50	306.60	32.6	1.3	335	2	647	6	17.7	0.1	114	1	1.35	0.01	3.30	0.15
37X-1	313.12	313.22	32.9	1.2	331	2	682	8	18.9	0.1	116	1	1.42	0.02	3.78	0.13
38X-5	328.30	328.40	32.3	1.3	326	3	728	7	20.8	0.2	113	1	1.46	0.02	3.61	0.14
39X-5	337.71	337.81	34.0	1.3	332	3	768	9	22.4	0.2	116	1	1.48	0.02	3.38	0.15
40X-1	341.50	341.60	33.0	1.3	312	2	783	9	21.7	0.2	114	1	1.41	0.02	3.43	0.12
41X-1	351.10	351.20	33.2	1.2	304	2	689	6	23.6	0.1	115	1	1.11	0.01	2.02	0.12
42X-2	362.20	362.30	32.6	1.3	306	4	902	7	21.9	0.2	114	1	1.39	0.02	2.96	0.20
44X-1	379.75	379.85	33.9	1.3	300	4	894	12	25.0	0.2	115	1	1.33	0.03	2.39	0.14
45X-3	392.45	392.55	38.9	1.2	304	2	941	6	30.4	0.2	114	1	1.40	0.02	2.67	0.14
49X-1	427.48	427.58	50.3	1.3	308	2	679	6	32.2	0.2	131	1	1.01	0.02	1.86	0.16

Sr values in bold are from inductively coupled plasma-optical emission spectrometry analysis at a higher dilution, as indicated in text.



Table T2. Composition of sediment digest, Sites U1395–U1400.

Core, section	Offset (cm)		Depth CSF-A (m)		Al	\pm	Ba	\pm	Ca	\pm	Cu	\pm	Fe	\pm	K	\pm	Mg	\pm	Mn	\pm	Na	\pm	Sr	\pm	Ti	\pm	V	\pm
	Top	Bottom	Top	Bottom	(wt%)	(wt%)	(ppm)	(ppm)	(wt%)	(wt%)	(ppm)	(ppm)	(wt%)	(wt%)	(wt%)	(wt%)	(wt%)	(ppm)	(ppm)	(wt%)	(ppm)	(wt%)	(ppm)	(wt%)	(ppm)	(wt%)	(ppm)	
340-U1395B-																												
1H-3	140	150	4.40	4.50	2.18	0.01	79	5	29.3	0.1	12.4	1.2	1.21	0.02	0.23	0.04	1.24	0.01	299	4	0.87	0.01	2272	8	0.10	0.00	42.5	1.6
6H-4	130	140	49.72	49.82	5.02	0.02	163	4	19.6	0.1	32.7	1.2	2.77	0.02	0.64	0.02	1.20	0.01	821	4	1.47	0.01	1772	10	0.24	0.00	76.0	1.4
13H-4	130	140	112.02	112.12	3.76	0.02	210	15	24.1	0.1	22.1	1.1	2.12	0.01	0.47	0.04	0.84	0.01	644	4	0.99	0.01	2042	10	0.17	0.00	69.2	1.7
14H-3	140	150	117.30	117.40	7.52	0.04	192	15	8.4	0.1	29.5	1.2	3.28	0.02	0.72	0.03	1.33	0.01	924	4	2.55	0.01	547	3	0.26	0.00	95.1	1.5
14H-3	140	150	117.30	117.40	7.66	0.05	195	15	8.5	0.1	31.3	1.5	3.30	0.02	0.73	0.05	1.35	0.01	918	7	2.59	0.03	555	3	0.26	0.00	95.9	1.6
24X-1	140	150	185.50	185.60	2.49	0.03	98	5	27.9	0.1	18.1	1.2	1.20	0.02	0.31	0.03	0.80	0.01	553	5	0.90	0.01	2533	10	0.10	0.00	44.7	2.2
25X-1	140	150	195.10	195.20	4.29	0.03	245	15	22.6	0.2	23.4	1.2	1.86	0.02	0.67	0.03	0.81	0.01	473	5	0.97	0.01	2267	14	0.17	0.00	64.5	2.4
340-U1396C-																												
1H-3	140	150	4.40	4.50	3.63	0.03	161	4	26.1	0.1	14.4	1.3	1.98	0.02	0.38	0.05	0.64	0.01	339	4	1.15	0.01	1709	8	0.16	0.00	84.4	1.5
2H-3	140	150	12.80	12.90	4.19	0.03	132	5	24.0	0.1	13.4	1.3	2.00	0.02	0.43	0.02	0.66	0.01	497	5	1.26	0.01	961	7	0.16	0.00	64.3	1.8
2H-3	140	150	12.80	12.90	4.16	0.03	130	4	23.5	0.1	19.5	1.4	1.94	0.02	0.47	0.02	0.63	0.01	468	3	1.26	0.01	952	8	0.17	0.00	61.8	2.0
8H-3	140	150	69.80	69.90	3.44	0.02	192	15	25.3	0.1	16.2	1.2	1.86	0.02	0.56	0.03	0.54	0.01	294	4	1.27	0.01	954	8	0.15	0.00	58.1	2.3
8H-6	142	152	74.35	74.45	3.70	0.03	183	4	25.5	0.3	13.5	1.2	2.12	0.02	0.50	0.03	0.57	0.01	382	4	1.22	0.01	983	13	0.16	0.00	60.7	1.5
14H-5	130	140	127.54	127.64	3.67	0.03	165	5	24.2	0.1	18.5	1.3	2.42	0.02	0.50	0.02	0.59	0.01	1010	6	1.46	0.02	908	8	0.21	0.00	68.2	2.3
15H-3	140	150	134.33	134.43	4.75	0.04	164	4	19.2	0.2	16.6	1.4	2.72	0.03	0.74	0.03	0.66	0.01	947	5	2.01	0.02	735	9	0.23	0.00	71.5	1.9
15H-6	140	150	138.80	138.90	5.38	0.07	190	4	14.2	0.1	32.3	1.1	3.65	0.04	0.84	0.03	0.80	0.01	1023	8	2.17	0.03	601	7	0.32	0.00	102.6	1.5
340-U1399B-																												
1H-2	140	150	2.90	3.00	7.56	0.06	376	15	4.2	0.0	91.4	1.2	2.30	0.02	1.94	0.03	0.73	0.01	755	5	2.64	0.02	275	2	0.17	0.00	52.8	1.5
2H-3	140	150	10.10	10.20	8.13	0.03	307	15	9.9	0.1	45.4	1.5	3.80	0.02	1.50	0.02	1.27	0.02	1051	6	1.78	0.01	723	8	0.34	0.00	130.0	2.3
6H-2	135	145	46.50	46.60	7.83	0.03	260	15	8.6	0.1	75.9	1.5	4.32	0.02	1.22	0.03	1.65	0.02	1100	5	1.99	0.01	563	3	0.35	0.00	133.1	1.7
6H-4	135	145	49.45	49.55	6.67	0.06	265	15	13.4	0.1	41.1	1.5	3.00	0.03	1.02	0.04	1.10	0.01	1183	8	1.68	0.02	976	9	0.24	0.00	86.9	1.6
6H-4	135	145	49.45	49.55	6.64	0.04	266	15	13.4	0.1	42.1	1.4	2.97	0.02	1.04	0.02	1.09	0.01	1172	6	1.64	0.01	977	9	0.24	0.00	87.6	1.5
18H-2	140	150	131.83	131.93	7.84	0.03	190	15	8.4	0.1	31.9	1.5	4.52	0.03	0.81	0.03	1.30	0.01	1281	6	2.03	0.01	550	2	0.44	0.00	122.0	1.6
24H-1	140	150	160.70	160.80	7.91	0.04	305	15	9.0	0.1	38.4	1.2	3.69	0.02	1.27	0.03	1.19	0.01	932	6	1.86	0.01	561	3	0.28	0.00	104.0	1.8
25H-1	140	150	167.80	167.90	7.15	0.08	292	15	12.0	0.1	45.8	1.2	3.42	0.04	1.27	0.02	1.43	0.01	1946	15	1.23	0.02	844	9	0.31	0.00	123.5	1.5
340-U1400B-																												
7H-4	140	150	31.24	31.34	6.89	0.03	236	15	13.9	0.1	43.9	1.2	3.70	0.02	1.11	0.03	1.17	0.01	1080	4	1.33	0.01	1049	7	0.32	0.00	129.4	1.7
8H-5	140	150	42.40	42.50	7.68	0.07	236	15	10.5	0.1	49.9	1.2	2.87	0.02	1.23	0.02	1.09	0.01	1370	9	1.60	0.02	785	7	0.25	0.00	96.5	1.6
27H-5	136	146	200.79	200.89	8.81	0.03	194	14	6.7	0.0	53.6	1.2	4.07	0.02	1.04	0.03	1.16	0.01	1155	4	2.37	0.01	402	2	0.32	0.00	122.5	1.6
28H-3	137	147	207.30	207.40	8.72	0.03	276	15	7.3	0.0	40.8	1.2	4.16	0.03	1.06	0.04	1.45	0.02	1446	8	2.09	0.02	428	2	0.32	0.00	125.2	1.9
340-U1400C-																												
33X-2	140	150	285.80	285.90	7.10	0.04	188	4	13.2	0.1	50.0	1.4	3.80	0.03	0.98	0.04	1.16	0.01	1127	7	1.36	0.01	977	8	0.35	0.00	125.5	1.4
41X-1	140	150	351.10	351.20	7.58	0.05	290	15	11.2	0.1	45.2	1.2	3.93	0.03	1.38	0.04	1.19	0.01	1395	6	1.05	0.02	676	7	0.34	0.00	128.4	1.4
49X-1	108	116	427.48	427.58	8.10	0.08	293	16	8.5	0.1	48.4	1.3	4.01	0.06	1.68	0.02	1.31	0.02	1264	16	1.27	0.02	514	5	0.38	0.00	147.7	1.6
Laboratory standard RR9702A-42MC (Chilean Margin sediment)																												
			Mean $\pm 1\sigma$	8.18	0.04	406	2	2.66	0.04	40.8	0.5	4.73	0.05	1.41	0.01	1.45	0.02	518	5	3.21	0.03	307	3	0.48	0.004	124	1	
			Number of samples (N)	5		5		5		5		5		5		5		5		5		5		5		5		
			Prior laboratory results	8.18	0.12	410	6	2.66	0.04	42.5	2	4.73	0.08	1.44	0.02	1.43	0.03	512	8	3.22	0.05	309	5	0.48	0.007	124	3	
			Number of samples (N)	38		38		38		38		38		32		38		38		32		38		38		38		
PACS-2																												
			Mean $\pm 1\sigma$	6.30	0.05	980	24	1.97	0.03	NR	NR	4.12	0.04	1.21	0.02	1.42	0.01	436	5	3.38	0.03	271	3	0.43	0.00	132	2	
			Number of samples (N)	5		5		5		5		5		5		5		5		5		5		5		5		
			Prior laboratory results	6.3	0.09	980	21	1.98	0.02	311	6	4.12	0.07	1.22	0.03	1.41	0.03	431	7	3.4	0.05	273	4	0.43	0.008	132		
			Number of samples (N)	38		38		38		38		38		32		38		38		32		38		38		38		
			Certified values	6.62	0.16			1.96	0.09	310	6	4.09	0.03	1.24	0.03	1.47	0.07	440	10	3.45	0.09	276	15	0.443	0.016	133	3	

NR = analyses for Cu on PACS-2 standard were outside the calibration and are not reported here.

Table T3. Inductively coupled plasma–optical emission spectrometry specifications.

Element	Line (nm)	View
Al	396.152	Radial
Ba	455.403	Radial
Ca	317.933	Radial
Cu	324.754	Axial
Fe	259.940	Radial
K	766.491	Radial
Mg	279.078	Axial
Mn	257.610	Radial
Na	589.592	Radial
Sr	407.771	Radial
Ti	334.941	Radial
V	292.401	Axial
Zn	206.200	Axial

Table T4. Composition of solid phases, Sites U1394–U1396, U1399, and U1400. (Continued on next two pages.)

Core, section	Offset (cm)		Depth CSF-A (m)		CaCO ₃ (wt%)	± (wt%)	TIC (wt%)	± (wt%)	OC (wt%)	N (wt%)	Fe _R (wt%)	± (wt%)	Mn _R (wt%)	± (wt%)
	Top	Bottom	Top	Bottom										
340-U1394A-														
1H-2	94	95	2.44	2.45							0.34		0.010	
1H-4	24	25	4.24	4.25	69.0		8.29		0.192	0.025	0.29		0.044	
2H-5	81	82	11.67	11.68							0.69		0.011	
2H-7	22	23	13.79	13.80	8.3		1.00		0.042	0.003	0.39		0.008	
3H-1	37	38	14.67	14.68	67.3		8.08		0.152	0.022	0.33		0.025	0.020
3H-3	43	44	17.73	17.74	34.1		4.09		0.050	0.006	0.42		0.023	
3H-6	73	74	22.53	22.54	35.0		4.20		0.043	0.006	0.50		0.018	
14X-1	80	81	111.20	111.21	62.6		7.51		0.190	0.025	0.33		0.036	
16X-1	48	49	130.08	130.09	12.5		1.50		0.210	0.026	0.36		0.022	
16X-2	63	64	131.69	131.70	58.5		7.02		0.267	0.032	0.35	0.23	0.022	0.029
17X-2	47	48	141.17	141.18	58.2		6.99		0.292	0.029	0.37	0.09	0.026	0.009
17X-5	122	123	146.42	146.43	59.0		7.08		0.355	0.036	0.30		0.015	
18X-1	44	45	149.24	149.25	37.2		4.47		0.115	0.018	0.37		0.042	
18X-3	71	72	152.51	152.52	56.4		6.77		0.300	0.033	0.41		0.029	
19X-1	52	53	158.92	158.93	61.2		7.34		0.155	0.021	0.37		0.030	
19X-2	67	68	160.57	160.58	55.2		6.62		0.420	0.043	0.36	0.01	0.019	0.000
20X-1	57	58	168.57	168.58	32.1		3.86		0.113	0.016	0.44	0.01	0.035	0.011
22X-1	21	22	187.31	187.32	54.5		6.55		0.183	0.024	0.35	0.01	0.043	0.001
23X-1	68	69	197.38	197.39	50.9		6.10		0.213	0.024	0.36	0.01	0.035	0.001
340-U1395A-														
1H-2	55	56	0.85	0.86	75.8		9.10		0.104	0.012	0.18		0.007	
2H-3	104	105	7.14	7.15	34.9		4.19		0.184	0.024	0.37		0.028	
2H-6	7	8	10.67	10.68	12.7		1.53		0.030	0.003	0.40	0.01	0.010	0.000
4H-4	96	97	25.36	25.37	45.1		5.41		0.094	0.015	0.71	0.01	0.031	0.000
6H-2	112	113	41.53	41.54	0.1		0.02		0.026	0.000	0.39	0.01	0.009	
6H-5	44	45	45.37	45.38	29.5		3.54		0.119	0.012	0.51	0.02	0.010	0.000
6H-6	91	92	47.35	47.36	12.2		1.46		0.108	0.013	0.48	0.01	0.018	0.000
7H-1	22	23	48.62	48.63	48.0		5.76		0.214	0.026	0.54	0.01	0.037	0.000
7H-2	135	136	51.25	51.26	29.5		3.54		0.138	0.012	0.50	0.01	0.009	0.000
7H-6	26	27	55.74	55.75	45.3		5.43		0.069	0.007	0.37	0.01	0.008	0.000
8H-1	18	19	57.28	57.29	46.7		5.60		0.253	0.031	0.51	0.03	0.020	0.001
8H-3	13	14	60.23	60.24	54.0		6.49		0.234	0.022	0.39	0.02	0.019	0.000
9H-4	134	135	68.77	68.78	9.8		1.18		0.087	0.008	0.75		0.008	
9H-6	110	111	71.55	71.56	44.5		5.34		0.109	0.013	0.35		0.019	
10H-3	67	68	76.07	76.08	1.9		0.23		0.053	0.004	0.51		0.006	
10H-4	69	70	77.59	77.60	43.3		5.19		0.147	0.021	0.45		0.032	
11H-2	103	104	82.93	82.94	54.5		6.55		0.209	0.012	0.39		0.091	
11H-6	33	34	88.28	88.29	53.6		6.43		0.166	0.024	0.34		0.039	
12H-3	130	131	94.20	94.21	37.4		4.49		0.064	0.008	0.24		0.011	
12H-4	78	79	95.19	95.20	4.1		0.49		0.014	0.002	0.39	0.04	0.005	0.000
12H-7	46	47	99.38	99.39	35.7		4.28		0.082	0.014	0.45		0.034	
14H-1	60	61	109.50	109.51	68.6		8.24		0.263	0.030	0.23		0.013	
14H-3	16	17	112.06	112.07	43.5		5.22		0.093	0.011	0.20		0.009	
18X-1	39	40	135.99	136.00	55.4		6.65		0.239	0.031	0.33		0.017	
18X-3	58	59	139.18	139.20	5.7		0.69		0.166	0.013	0.70		0.004	
22X-1	39	40	169.29	169.30	81.1		9.74		0.148	0.016	0.21		0.031	
25X-1	49	50	193.49	193.50			0.00				0.000	0.21		0.012
26X-1	59	60	203.19	203.20	62.3		7.48		0.169	0.021	0.38		0.022	
26X-2	6	7	204.09	204.10	65.5		7.86		0.103	0.012	0.36		0.021	
27X-1	48	49	212.58	212.60			0.00				0.000	0.28		0.016
28X1	74	75	222.44	222.50	43.5		5.22		0.210	0.016	0.29		0.013	
340-U1396A-														
1H-1	77	78	0.77	0.78	59.6		7.15		0.089	0.015	0.37	0.01	0.011	0.000
1H-4	78	79	5.28	5.29	56.2		6.75		0.062	0.009	0.36		0.013	
3H-1	120	121	16.30	16.31	42.3		5.07		0.074	0.011	0.43		0.011	
3H-4	100	101	20.60	20.61	62.8		7.54		0.063	0.011	0.27	0.00	0.012	0.000
3H-6	56	57	23.16	23.17	72.4		8.69		0.072	0.012	0.32		0.012	
4H-2	63	64	26.73	26.74	32.2		3.86		0.097	0.012	0.39		0.007	
4H-4	95	96	30.05	30.06	60.4		7.25		0.153	0.015	0.32		0.013	
4H-6	24	25	32.34	32.35	35.5		4.26		0.105	0.013	0.34		0.009	
5H-1	51	52	34.61	34.62	13.4		1.61		0.032	0.004	0.40	0.01	0.005	0.000
5H-4	87	88	39.47	39.48	73.1		8.77		0.099	0.015	0.33		0.012	
6H-2	97	97	46.07	46.08	0.0		0.00		0.000	0.000	0.34		0.014	
6H-6	102	103	52.12	52.13	59.1		7.10		0.184	0.022	0.38		0.011	
7H-2	89	90	55.49	55.50	53.2		6.39		0.149	0.018	0.37	0.02	0.014	0.001



Table T4 (continued). (Continued on next page.)

Core, section	Offset (cm)		Depth CSF-A (m)		CaCO ₃ (wt%)	± (wt%)	TiC (wt%)	± (wt%)	OC (wt%)	N (wt%)	Fe _R (wt%)	± (wt%)	Mn _R (wt%)	± (wt%)
	Top	Bottom	Top	Bottom										
7H-6	69	70	61.29	61.30	27.9		3.35		0.129	0.013	0.42		0.008	
8H-5	91	92	69.52	69.53	69.1		8.29		0.130	0.017	0.25		0.015	
9H-2	119	120	74.81	74.82	64.1		7.70		0.130	0.018	0.25		0.017	
9H-7	56	57	81.64	81.65	58.9		7.07		0.218	0.026	0.28		0.016	
10H-1	81	82	82.41	82.42	65.8		7.90		0.188	0.022	0.29		0.024	
10H-5	74	75	88.30	88.31	58.4		7.01		0.175	0.022	0.27		0.020	
11H-1	83	84	91.93	91.94	42.9		5.15		0.156	0.020	0.46		0.021	
11H-7	55	56	100.49	100.50	31.2		3.74		0.168	0.017	0.48		0.021	
12H-1	44	45	101.04	101.05	50.4		6.05		0.181	0.021	0.37		0.023	
13H-1	47	48	107.77	107.78	33.9		4.07		0.140	0.016	0.36		0.029	
13H-5	85	86	114.15	114.16	44.9		5.39		0.197	0.020	0.30		0.029	
14H-1	95	96	116.85	116.86	43.0		5.16		0.064	0.009	0.39		0.027	
14H-6	113	114	124.54	124.55	63.6		7.63		0.214	0.023	0.28		0.042	
15H-2	105	106	127.95	127.96	51.8		6.22		0.153	0.018	0.34		0.051	
15H-6	33	34	133.25	133.26	40.0		4.80		0.107	0.014	0.45		0.035	
340-U1399A-														
1H-1	73	74	0.73	0.74	30.8		3.70		0.279	0.051	0.66		0.025	
1H-2	9	10	1.59	1.60	2.6		0.31		0.033	0.006	0.46		0.006	
2H-4	112	113	10.72	10.73	20.9		2.51		0.420	0.062	0.77		0.054	
2H-6	29	30	12.89	12.90	33.2		3.98		0.286	0.036	0.64		0.047	
3H-1	69	70	15.29	15.30	4.5		0.54		0.026	0.006	0.41		0.009	
3H-3	46	47	18.06	18.07	30.0		3.60		0.229	0.047	0.78		0.076	
4H-2	85	86	26.45	26.46	7.8		0.94		0.152	0.027	0.65	0.03	0.030	0.005
4H-4	105	106	29.65	29.66	20.9		2.50		0.293	0.056	1.20	0.04	0.088	0.000
5H-3	10	11	36.70	36.71	22.6		2.71		0.460	0.068	0.94		0.099	
5H-5	133	134	40.94	40.95	9.3		1.12		0.504	0.074	1.66		0.268	
6H-1	69	70	43.79	43.80	26.6		3.19		0.318	0.060	0.75	0.03	0.086	0.002
6H-6	123	124	51.63	51.64	17.4		2.09		0.390	0.057	1.06		0.070	
7H-1	101	102	53.61	53.62	34.7		4.16		0.458	0.063	0.61		0.072	
7H-5	114	115	59.74	59.75	17.5	0.1	2.11	0.01	0.279	0.041	0.82		0.047	
8H-1	44	45	62.54	62.55	27.2		3.26		0.297	0.043	0.79		0.068	
9H-4	129	130	76.61	76.62	14.7		1.76		0.322	0.051	1.03		0.057	
9H-7	14	15	79.96	79.97	11.1		1.33		0.582	0.080	1.16		0.047	
10H-2	102	103	82.82	82.83	14.5		1.75		0.329	0.055	1.40		0.093	
10H-5	60	61	86.85	86.86	3.7		0.45		0.614	0.080	1.40	0.01	0.053	0.002
11H-1	43	44	90.23	90.24	7.6	0.0	0.91	0.01	0.058	0.010	0.67		0.026	
12H-3	36	37	94.29	94.30	2.2		0.26		0.025	0.006	0.64		0.010	
13H-1	60	61	95.70	95.71	24.2	0.2	2.91	0.02	0.216	0.039	0.70		0.063	
14H-1	52	53	103.42	103.43	26.6	2.0	3.20	0.24	0.461	0.064	0.76		0.071	
14H-2	59	60	104.99	105.00	8.3		1.00		0.042	0.007	0.42		0.013	
15H-2	59	60	114.09	114.10	35.6	0.0	4.27	0.00	0.471	0.069	0.49		0.110	
16H-4	45	46	126.40	126.41	14.3		1.71		0.266	0.036	0.68		0.117	
17H-3	95	96	134.91	134.92	11.1	0.1	1.33	0.00	0.141	0.019	0.65		0.053	
17H-7	12	13	140.02	140.03	24.1		2.89		0.384	0.055	0.64	0.01	0.083	0.000
18H-1	55	56	141.05	141.06	20.1		2.41		0.308	0.049	0.81		0.150	
20H-1	100	101	154.40	154.41	14.2		1.70		0.322	0.050	0.84		0.049	
20H-4	39	40	158.29	158.30	21.1		2.54		0.317	0.041	0.91		0.170	
23H-1	62	63	167.82	167.83	20.6	0.2	2.48	0.02	0.239	0.031	0.92		0.073	
23H-5	129	130	174.45	174.46	23.1	0.3	2.77	0.03	0.274	0.045	0.75		0.052	
24H-1	38	39	175.78	175.79	17.4		2.08		0.339	0.048	1.01		0.064	
25H-1	70	71	185.20	185.21	21.8		2.62		0.338	0.056	0.88	0.01	0.049	0.002
26H-1	15	16	191.85	191.86	33.2		3.99		0.256	0.050	0.56		0.075	
26H-3	80	81	195.54	195.55	2.1		0.25		0.055	0.015	0.85		0.008	
27H-1	78	79	198.48	198.49	20.6		2.47		0.353	0.058	1.06	0.15	0.048	0.004
27H-4	32	33	202.56	202.57	26.1		3.13		0.368	0.053	0.64		0.060	
28H-2	18	19	205.06	205.07	17.8		2.13		0.271	0.045	0.94		0.039	
29H-1	72	73	206.22	206.23	29.5		3.54		0.199	0.036	0.77		0.069	
31X-1	77	78	217.87	217.88	30.8		3.70		0.170	0.047	0.65		0.086	
33X-1	95	96	237.25	237.26	25.5		3.06		0.329	0.045	0.74		0.047	
34X-CC	20	21	246.83	246.84	12.1		1.46		0.076	0.009	0.61		0.026	
35X-CC	16	17	256.25	256.26	16.1		1.93		0.068	0.010	0.55		0.019	
36X-2	57	58	267.17	267.18	21.4		2.56		0.087	0.016	0.47		0.040	
36X-3	98	99	269.08	269.09	22.3	0.0	2.68	0.01	0.457	0.072	0.75		0.099	
340-U1400B-														
1H-1	19	20	0.19	0.20	18.6		2.23		0.400	0.052	0.88		0.023	
1H-2	105	106	2.55	2.56	9.8				0.162	0.022	0.92		0.024	
7H-3	51	52	28.85	28.86	34.6				0.327	0.040	0.60		0.054	
7H-6	65	66	33.49	33.50	24.5	0.1	2.94	0.01	0.270	0.027	0.60		0.037	

Table T4 (continued).

Core, section	Offset (cm)		Depth CSF-A (m)		CaCO ₃ (wt%)	± (wt%)	TIC (wt%)	± (wt%)	OC (wt%)	N (wt%)	Fe _R (wt%)	± (wt%)	Mn _R (wt%)	± (wt%)
	Top	Bottom	Top	Bottom										
10H-1	88	89	49.38	49.39	23.5		2.82		0.309	0.047	0.89		0.089	
10H-5	52	53	55.03	55.04	22.8	0.3	2.71		0.247	0.040	0.78		0.145	
11H-2	103	104	60.53	60.54	11.6		1.39		0.270	0.040	1.20	0.03	0.049	0.001
11H-7	30	31	66.92	66.93	17.6	0.1	2.12	0.01	0.133	0.019	0.86		0.069	
15H-2	93	94	95.39	95.40	22.1		2.65		0.270	0.044	0.81		0.086	
15H-5	63	64	99.53	99.54	23.4	0.5	2.81	0.06	0.294	0.044	0.87		0.094	
17H-1	123	124	106.93	106.94	19.9		2.39		0.291	0.040	0.81		0.065	
17H-5	80	81	112.43	112.44	4.9		0.59		0.099	0.014	1.23		0.021	
18H-3	53	54	118.67	118.68	6.9		0.82		0.207	0.020	1.09		0.035	
18H-7	57	58	124.59	124.60	15.7		1.88		0.235	0.029	0.81		0.053	
19H-3	60	61	128.22	128.23	14.0		1.68		0.248	0.036	1.07		0.060	
20H-4	108	109	134.39	134.40	12.6		1.51		0.152	0.020	0.97		0.046	
21H-1	110	111	137.70	137.71	20.7		2.48		0.239	0.043	1.07		0.177	
21H-5	34	35	142.79	142.80	13.7		1.65		0.263	0.022	0.74	0.04	0.049	0.002
22H-1	115	116	147.25	147.26	13.5	0.4	1.62	0.05	0.142	0.027	0.68		0.062	
22H-7	32	33	155.03	155.04	19.7	0.9	2.37	0.10	0.265	0.044	0.62		0.101	
23H-2	90	91	157.96	157.97	24.6		2.95		0.153	0.030	0.53	0.02	0.086	0.001
23H-7	13	14	164.08	164.09	20.2	0.0	2.43	0.00	0.218	0.043	0.79	0.00	0.073	0.001
24H-2	40	41	166.97	166.98	32.4	0.5	3.89	0.05	0.242	0.037	0.64		0.108	
24H-6	67	69	173.12	173.14	25.0		3.00		0.209	0.038	0.68		0.106	
25H-2	58	59	176.64	176.65	34.3		4.12		0.186	0.039	0.51		0.149	
25H-6	28	29	182.20	182.21	27.4		3.29		0.206	0.040	0.62		0.126	
26H-2	48	49	185.95	185.96	8.2		0.98		0.151	0.017	0.76		0.026	
26H-7	75	76	193.58	193.59	7.7		0.92		0.136	0.017	0.78		0.050	
27H-1	62	63	194.12	194.13	4.4	0.2	0.53	0.02	0.177	0.019	1.42		0.022	
28H-2	53	54	204.99	205.00	12.6	0.1	1.51	0.01	0.258	0.031	0.68	0.00	0.062	0.001
28H-6	33	34	210.65	210.66	2.1	0.1	0.25	0.01	0.096	0.010	1.06		0.017	
340-U1400C-														
10H-1	60	61	79.30	79.31	8.3		1.00		0.158	0.024	0.78		0.029	
11H-1	116	117	85.96	85.97	18.6	0.4	2.23	0.05	0.225	0.032	0.72		0.078	
12H-2	25	26	95.55	95.56	14.1	0.3	1.69	0.03	0.218	0.029	0.73		0.040	
13H-6	7	8	110.90	110.91	16.4		1.96		0.301	0.042	0.57		0.041	
22H-4	43	44	186.42	186.43	10.0		1.20		0.097	0.018	0.54		0.015	
27X-2	96	97	227.76	227.77	7.9		0.95		0.240	0.027	0.93		0.039	
28X-1	52	53	235.42	235.43	6.7		0.81		0.141	0.014	0.86		0.105	
29X-2	50	51	246.50	246.51	18.8		2.26		0.336	0.041	0.72		0.027	
30X-1	31	32	254.41	254.42	23.6	0.5	2.85	0.08	0.258	0.034	0.61		0.091	
31X-1	21	22	263.91	263.92	13.0		1.56		0.147	0.022	0.79		0.042	
32X-3	122	123	277.52	277.53	27.7		3.32		0.331	0.035	0.89		0.102	
33X-3	33	34	286.23	286.24	25.6		3.07		0.340	0.036	0.79		0.076	
35X-3	49	50	295.99	296.00	18.6		2.23		0.398	0.035	1.04	0.01	0.054	0.002
36X-2	113	114	304.73	304.74	23.4		2.81		0.185	0.028	0.79		0.068	
37X-2	21	22	313.43	313.44	21.5	0.3	2.58	0.04	0.347	0.048	0.89	0.06	0.072	0.001
38X-1	111	112	322.01	322.02	31.4		3.77		0.352	0.045	0.74		0.089	
38X-6	98	99	329.38	329.39	7.6		0.91		0.137	0.014	0.83		0.031	
39X-2	77	78	332.77	332.78	24.0		2.87		0.216	0.030	0.61		0.140	
40X-1	94	95	341.04	341.05	9.3		1.11		0.140	0.016	0.75		0.032	
41X-1	115	116	350.85	350.86	25.0		3.00		0.265	0.039	0.61		0.082	
42X-2	66	67	361.46	361.47	9.8		1.17		0.099	0.013	0.81		0.028	
43X-1	46	47	369.36	369.37	10.8	1.0	1.30	0.12	0.106	0.012	0.89	0.01	0.056	0.000
44X-2	72	73	380.57	380.58	17.4		2.09		0.195	0.026	0.72		0.046	
45X-4	40	41	392.95	392.96	15.3		1.84		0.207	0.028	0.82		0.062	
46X-1	35	36	397.95	397.96	16.1	0.2	1.93	0.03	0.336	0.037	0.76	0.01	0.057	0.000
47X-1	65	66	407.85	407.86	22.0		2.64		0.212	0.032	0.54		0.081	
48X-CC	13	14	417.46	417.47	34.0		4.08		0.312	0.041	0.41		0.136	
49X-1	61	62	427.01	427.02	25.7	1.1	3.08	0.13	0.310	0.041	0.51		0.114	

TIC = total inorganic carbon, OC = organic carbon. Fe_R = dithionite-extractable iron, Mn_R = dithionite-extractable manganese.

Table T5. Composition of solid phases in high-resolution sections, Sites U1399 and U1400. (Continued on next page.)

Core, section	Offset (cm)		Depth CSF-A (m)		CaCO ₃ ± (wt%)	TIC ± (wt%)	OC ± (wt%)	N ± (wt%)	Fe _R ± (wt%)	Mn _R ± (wt%)	Lithology descriptions
	Top	Bottom	Top	Bottom	(wt%)	(wt%)	(wt%)	(wt%)	(wt%)	(wt%)	
340-U1399B-											
3H-3	88	90	19.08	19.10	9.2	1.10	0.206	0.031	1.13	0.06	Mud with hints of silt/very fine grained sand
	93	95	19.13	19.15	5.7	0.1	0.68	0.01	0.143	0.05	Very fine sand/silt with some mud present
	98	100	19.18	19.20	11.7	1.41	0.241	0.032	0.80	0.06	Very fine sand/silt with some mud present
	101	103	19.21	19.23	7.2	0.0	0.86	0.00	0.072	0.03	Fine-grained sand
	104	106	19.24	19.26	41.4	0.1	4.96	0.01	0.288	0.07	35%–40% shell fragments, 60%–65% fine-grained sand/silt
	108	110	19.28	19.30	16.8	0.3	2.01	0.03	0.283	0.13	Mud
7H-3	17	19	56.37	56.39	13.4	0.5	1.61	0.06	0.273	0.09	Mud with hint of silt
	21	23	56.41	56.43	11.4	1.37	0.260	0.037	1.15	0.08	Mud
	25	27	56.45	56.47	15.6	0.2	1.88	0.03	0.265	0.11	Mud with silt
	30	32	56.50	56.52	17.6	2.12	0.215	0.041	0.94	0.00	Mud with hints of silt
	34	36	56.54	56.56	21.5	0.1	2.58	0.02	0.261	0.11	Mud with hints of silt
	65	67	56.85	56.87	20.3	2.44	0.203	0.032	0.75	0.14	Mud with hints of silt
	68	70	56.88	56.90	22.9	2.75	0.272	0.038	0.82	0.02	2% very fine grained sand, mud
	73	75	56.93	56.95	17.5	0.6	2.10	0.07	0.144	0.08	Fine–very fine grained sand 50%–75%, 25%–50% mud
	76	78	56.96	56.98	17.3	0.1	2.07	0.01	0.208	0.10	Mud
	81	83	57.01	57.03	13.5	0.1	1.63	0.01	0.179	0.10	Silt/very fine grained sand dominates, clay is present
11H-2	79	81	92.09	92.11	5.9	0.1	0.70	0.02	0.083	0.03	<1% sand, 25%–30% tephra, 70%–74% mud/silt
	81	83	92.11	92.13	21.1	0.9	2.54	0.10	0.253	0.07	<1% sand, 5%–10% tephra, 89%–94% mud
	83	85	92.13	92.15	10.8	1.30	0.147	0.019	0.61	0.05	<1% sand, 10% tephra, 89% silty/mud
	87	89	92.17	92.19	17.1	0.1	2.05	0.01	0.179	0.00	Mud with hints of silt
	92	94	92.22	92.24	16.8	2.02	0.165	0.025	0.81	0.02	2% sand, <1% tephra, 97% mud with hints of silt
	96	98	92.26	92.28	4.3	0.2	0.52	0.02	0.121	0.02	10%–15% tephra, silt/fine sand, minimal mud
16H-2	24	26	125.94	125.96	11.5	1.39	0.249	0.032	0.93	0.08	Mud, <1% medium-grained sand
	28	30	125.98	126.00	6.2	0.0	0.74	0.00	0.184	0.07	<1% medium sand, mud with hints of silt
	32	34	126.02	126.04	8.4	0.1	1.01	0.01	0.180	0.07	Muddy sand, sand is very fine to fine grained
	36	38	126.06	126.08	15.5	0.3	1.86	0.04	0.310	0.26	Mud with hints of silt
	41	43	126.11	126.13	10.4	1.25	0.219	0.032	1.12	0.14	Mud with minor amounts of silt
19H-2	49	51	135.59	135.61	22.4	2.69	0.297	0.054	0.83	0.14	Mud with hints of silt
	52	54	135.62	135.64	20.4	0.2	2.45	0.03	0.337	0.10	Mud with hints of silt
	57	59	135.67	135.69	30.2	0.5	3.62	0.07	0.174	0.08	Fine sand with hints of mud
	62	64	135.72	135.74	26.5	0.2	3.18	0.03	0.137	0.07	Very fine to fine-grained sand with hints of mud
	68	70	135.78	135.80	26.3	0.6	3.15	0.08	0.140	0.08	Silty/sand with minimal mud
	71	73	135.81	135.83	18.6	0.1	2.23	0.01	0.243	0.01	Mud
25H-2	94	96	168.84	168.86	16.0	0.1	1.92	0.01	0.175	0.14	Mud
	98	100	168.88	168.90	15.5	0.0	1.86	0.00	0.103	0.17	Mud with hints of silt
	103	105	168.93	168.95	3.9	0.1	0.47	0.01	0.068	0.10	Very fine sand to silt of weathered tephra
	109	111	168.99	169.01	0.1	0.1	0.01	0.01	0.046	0.00	Very fine sand to silt of weathered tephra
	114	116	169.04	169.06	21.5	0.0	2.58	0.00	0.209	0.18	Mud with hints of silt
340-U1400B-											
16H-2	33	34	104.17	104.18	1.0	0.0	0.12	0.01	0.141	0.01	Medium/coarse sand
	37	38	104.21	104.22	0.8	0.3	0.10	0.03	0.021	0.01	Medium/fine sand with tephra present
	42	43	104.26	104.27	1.2	0.1	0.15	0.01	0.062	0.02	Mud with <5% medium sand
	46	47	104.30	104.31	6.5	0.1	0.78	0.02	0.098	0.04	Mud with <2% fine sand
	50	51	104.34	104.35	3.8	0.1	0.46	0.01	0.080	0.04	Mud with 2% fine/medium sand
	55	56	104.39	104.40	0.5	0.2	0.06	0.02	0.019	0.01	Medium-grained sand



Table T5. (continued).

Core, section	Offset (cm)		Depth CSF-A (m)		CaCO_3	\pm	TIC	\pm	OC	\pm	N	\pm	Fe_R	\pm	Mn_R	\pm	Lithology descriptions
	Top	Bottom	Top	Bottom	(wt%)	(wt%)	(wt%)	(wt%)	(wt%)	(wt%)	(wt%)	(wt%)	(wt%)	(wt%)	(wt%)	(wt%)	
26H-5	48	49	190.36	190.37	17.9		2.15		0.149		0.024		0.84		0.16		Mud
	53	54	190.41	190.42	14.6	0.2	1.75	0.02	0.092		0.015		0.74		0.12		50% mud, 50% very fine to fine-grained sand
	57	58	190.45	190.46	16.7	0.1	2.00	0.01	0.130		0.022		0.80	0.00	0.15	0.00	Mud
	61	62	190.49	190.50	10.1	0.3	1.21	0.03	0.128		0.018		1.04		0.10		Mud with silt present
	66	67	190.54	190.55	2.5	0.1	0.30	0.01	0.091		0.012		1.23	0.09	0.05	0.00	Mud--> volcaniclastic mud according to cruise
340-U1400C-48X-1	14	15	416.94	416.95	1.3	0.1	0.15	0.15	0.105		0.014		1.06		0.03		Mud/mudstone with some silt
	18	19	416.98	416.99	3.2	0.2	0.38	0.03	0.074		0.013		0.74		0.05		Mud/mudstone with minor silt
	22	23	417.02	417.03	2.1	0.1	0.26	0.01	0.064	0.016	0.007	0.002	0.44		0.03		20%–30% very fine to fine-grained sand, mud/silt
	25	26	417.05	417.06	2.5	0.1	0.30	0.01	0.076	0.003	0.011	0.001	0.23		0.04		Silty mud
	29	30	417.09	417.10	1.6	0.1	0.19	0.01	0.046	0.003	0.006	0.002	0.42	0.02	0.02	0.00	50% sand, 50% silty/mud, tephra present? <1%
	39	40	417.19	417.20	25.0	0.2	3.01	0.02	0.241		0.039		0.79		0.48		Mud

TIC = total inorganic carbon, OC = organic carbon. Fe_R = dithionite-extractable iron, Mn_R = dithionite-extractable manganese.



Table T6. Dithionite-extractable metals from Site U1396 ash layers.

Core, section	Offset (cm)		Fe (wt%)	± (wt%)	Mn (wt%)	± (wt%)	Al (wt%)	± (wt%)	OC (wt%)	± (wt%)	TIC (wt%)
	Top	Bottom									
340-U1396C-											
1H-2	51	52	0.39		0.0052		0.030		0.06		3.18
1H-3	79	80	0.55		0.0080				0.14		0.33
2H-1	76	77	0.43		0.0043		0.025		0.02		0.73
2H-7	64	65	0.83		0.0056		0.070		0.08		0.39
3H-2	59	60	0.57		0.0057		0.041		0.04		0.83
4H-6	42	43	0.39		0.0068		0.057		0.09		2.10
6H-2	94	95	0.70	0.02	0.0074	0.0005	0.062	0.000	0.17		0.55
6H-5	17	18	0.80		0.0064				0.10		0.24
8H-5	33	34	0.64	0.02	0.0049	0.0009	0.055		0.20	0.04	0.18
8H-5	41	42	0.40		0.0146		0.039		0.10		0.29
10H-6	131	132	0.76		0.0135		0.047		0.10		0.18
11H-2	104	105	0.52		0.0042		0.020		0.07	0.00	0.15
11H-2	107	108	0.48		0.0043		0.016		0.04		0.02
11H-4	90	91	0.58		0.0129		0.045		0.17		1.33
12H-1	118	119	0.36		0.0123		0.044		0.16		1.33
12H-3	127	128	0.82		0.0067		0.064		0.11		1.74
12H-3	130	131	1.26		0.0079		0.082		0.11		0.23
12H-4	21	22	0.66		0.0098		0.059		0.17		0.61
12H-4	39	40	0.77		0.0124		0.053		0.07		0.55
13H-6	139	140	0.34		0.0040		0.019		0.04		0.40
13H-7	44	45	0.32	0.01	0.0038	0.0002	0.017	0.000	0.04		0.03
14H-1	49	50	1.35	0.03	0.0147	0.0004	0.085	0.001	0.13	0.02	0.28
14H-3	40	41	0.38		0.0060				0.25		0.09
14H-3	87	88	0.39	0.00	0.0181	0.0000	0.044	0.001	0.12		1.35
14H-4	145	146	0.63		0.0088		0.080		0.18		0.34
15H-1	20.5	21.5	0.86		0.0157		0.078		0.09		0.72
15H-1	73	74	0.94		0.0112		0.102		0.08		0.20
15H-2	11	12	1.06		0.0142		0.096		0.13		0.63
15H-3	58	59	0.68		0.0144		0.065		0.15		0.86
15H-4	40	41	1.03		0.0112		0.064		0.05		0.10
15H-6	1	2	0.70		0.0264		0.052		0.15		1.60
15H-7	54	55	0.58		0.0067		0.040		0.07		0.10
15H-7	64	65	0.44		0.0100				0.12		0.23

OC = organic carbon, TIC = total inorganic carbon.

